(12)

NAVSWC TR 91-506

PVDF PRESSURE TRANSDUCERS FOR SHOCK WAVE AND EXPLOSIVES RESEARCH

BY PAUL GUSTAVSON DOUGLAS TASKER JERRY FORBES

WEAPONS RESEARCH AND TECHNOLOGY DEPARTMENT

16 FEBRUARY 1994

Approved for public release; distribution is unlimited.

NSWC
Naval Surface Warfare Center
DAHLGREN DIVISION

NAVAL SURFACE WARFARE CENTER
DAHLGREN DIVISION • WHITE OAK DETACHMENT
Silver Spring, Maryland 20903-5640

NAVSWC TR 91-506

PVDF PRESSURE TRANSDUCERS FOR SHOCK WAVE AND EXPLOSIVES RESEARCH

BY PAUL GUSTAVSON DOUGLAS TASKER JERRY FORBES
WEAPONS RESEARCH AND TECHNOLOGY DEPARTMENT

16 FEBRUARY 1994

NAVAL SURFACE WARFARE CENTER
DAHLGREN DIVISION • WHITE OAK DETACHMENT
Silver Spring, Maryland 20903-5640

FOREWORD

This work was performed for and funded by the Office of Naval Technology as part of the Explosives Project within the Explosives and Undersea Warheads Technology Block Program PE602314N. The results and conclusions in this report will be of interest to those seeking information on pressure gauges for use in underwater free field experiments, on structures, in explosive tests, and in explosive flyer plate designs.

Dr. R. Doherty and L. Roslund have given funding support for this work. M. Frankel (Defense Nuclear Agency) funded the research on the low inductance gauge reported in Appendix A. Gerrit Sutherland provided the manganin gauge record for the experiment on PBXW-123. E. R. Lemar and Gerrit Sutherland conducted one-dimensional code calculations for the explosive flyer plate experiment.

Approved by:

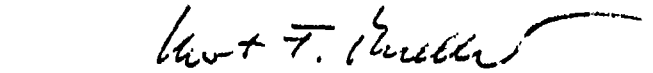

KURT F. MUELLER, Head
Explosives and Warheads Division

ABSTRACT

A polyvinylidene fluoride (PVDF) piezoelectric pressure transducer is described in this report. Techniques for its use and experimental applications are described in detail.

CONTENTS

Chapter		Page
1	INTRODUCTION	1-1
2	PVDF TRANSDUCER ELEMENTS	2-1
3	TECHNIQUES	3-1
4	EXPERIMENTAL APPLICATIONS OF PVDF SHOCK TRANSDUCERS	4-1
5	DISCUSSION AND CONCLUSIONS	5-1
	REFERENCES	6-1
	DISTRIBUTION	(1)

Appendix		Page
A	LOW INDUCTANCE PVDF SENSOR DESIGN	A-1

ILLUSTRATIONS

Figure		Page
2-1	THE STANDARDIZED ISL/BAUER PVDF TRANSDUCER ELEMENT	2-3
2-2	SHOCK RESPONSE CHARACTERIZATION DATA FOR ISL/BAUER PVDF	2-4
3-1	PVDF TRANSDUCER IN A CHARGE MODE CIRCUIT	3-2
3-2	PVDF TRANSDUCER IN A CURRENT MODE CIRCUIT	3-4
3-3	ERROR IN CURRENT MODE DATA CAUSED BY LOW DIGITIZER SENSITIVITY	3-7
4-1	EXPERIMENTAL ARRANGEMENT TO MEASURE STRESS AT A WATER/SOLID INTERFACE	4-2
4-2	PRESSURE-DISTANCE CALIBRATION OF A CYLINDRICAL PENTOLITE DONOR IN WATER	4-3
4-3	PVDF TRANSDUCER CIRCUIT PACKAGING	4-5
4-4	GRAPHICAL IMPEDANCE MISMATCH CALCULATION	4-6
4-5	SIGNAL FROM PVDF AT THE WATER/PMMA INTERFACE	4-7
4-6	SIGNAL FROM THE PVDF TRANSDUCER AT THE WATER/ALUMINUM INTERFACE	4-9
4-7	STRESS AT THE WATER/ALUMINUM INTERFACE	4-9
4-8	EXPERIMENTAL ARRANGEMENT TO MEASURE THE IMPULSE FROM A REACTING CYLINDER OF PBXW-123	4-11
4-9	CHARGE MODE AND CURRENT MODE RECORDS FOR THE PBXW-123 IMPULSE EXPERIMENT	4-12
4-10	STRESS IN A REACTING CYLINDER OF PBXW-123 AT THREE ADJACENT GAUGE LOCATIONS	4-13
4-11	FLYER PLATE PERFORMANCE EXPERIMENTAL ARRANGEMENT	4-15
4-12	DOUBLE IMPACT FROM A SPALLING ALUMINUM FLYER PLATE	4-16
A-1	NAVSWC DOUBLE MALTESE-CROSS SENSOR	A-2
A-2	UNDERWATER SHOCK WAVE MEASURED WITH THE NAVSWC DOUBLE MALTESE-CROSS SENSOR	A-4

CHAPTER 1

INTRODUCTION

This report details the application of polyvinylidene fluoride (PVDF) pressure transducers to shock wave and explosives research at the White Oak Laboratory of the Naval Surface Warfare Center (NAVSWC). The work discussed here used the well characterized PVDF film material developed by Francois Bauer of the Institut de Reserches in Saint Louis, France (ISL). A large body of publications exists detailing the development and manufacture of this PVDF material.[1,2] This standardized stress gauge has been shown to respond to shock loading over a large stress range (0 to 60 GPa). It can provide a direct measure of stress-rate over time with high sensitivity. Bauer reported in 1981 that strong and well characterized electrical signals are obtained from shock-compressed PVDF and its co-polymers.[3] Since then, much work has been performed to develop high quality, reproducible PVDF film and a standardized PVDF stress gauge element. The transducers used in this study were manufactured by Metravib* and supplied by Ktech.** Chapter 2 briefly describes these PVDF transducers, their manufacture, and how they work. A very fast response PVDF gauge has also been designed and tested at NAVSWC. This gauge was poled using the "Bauer" process but had a very low parasitic inductance; i.e., 3 nH compared to 25 nH for the standardized gauge. The low inductance should facilitate the measurement of very short rise time shocks. This NAVSWC design is described in Appendix A.

When using any fast response piezoelectric stress gauge, special attention must be given to measuring circuits and recording equipment. Chapter 3 covers gauge circuits and signal conditioning techniques.

We have used the standardized "Bauer" PVDF gauges in several research projects at NAVSWC. Chapter 4 discusses these experiments and results. Experiments will be described where underwater shock measurements were made close to a detonating Pentolite charge; the stress was measured at the end of a cylindrical charge of PBXW-123; and the stress induced in a polymethylmethacrylate (PMMA) plate by the impact of an aluminum flyer plate was measured.

* Metravib, CDS, 64 Chemin Des Mouilles, BP 182, 69132 Ecully France.
** Ktech Corporation, 901 Pennsylvania Avenue, NE, Albuquerque, NM 87110.

CHAPTER 2

PVDF TRANSDUCER ELEMENTS

THE PVDF POLYMER

PVDF Gauge Manufacture

The degree of piezoelectric response of a PVDF film depends upon the processes used to manufacture it. As molten PVDF is extruded and cooled, a nonpolar "alpha phase" material is produced. Alpha phase PVDF consists of randomly arranged chains of carbon atoms with a pair of hydrogen atoms attached to every other carbon atom. A pair of fluorine atoms is attached to the other carbon atoms. Mechanical stretching of the film during extrusion generates a polar, so-called beta phase PVDF, with the carbon chains aligned in parallel strips and planes. The hydrogen and fluorine pairs are randomly located around the axis of the carbon chains. It is the beta phase material that is used to make piezoelectric film sensors.

After stretching, the film is metallized on both sides in a desired electrode pattern with a region of overlap defined as the active area of the sensor. The active area is then subjected to a large electric field which permanently rotates the hydrogen and fluorine pairs around the chain, opposing one another. The result is a highly sensitive, thin film stress gauge.

THE STANDARDIZED PVDF SHOCK TRANSDUCER ELEMENT

Standardization

Through a long-term collaborative effort between the ISL and Sandia National Laboratory, Albuquerque, a set of specific processes was developed for the production and characterization of high quality precision PVDF sensors for shock research.[2]

At Rhône-Poulenc, in France, it was found that biaxially stretching alpha phase film produces the highest quality of beta phase PVDF. Rhone-Poulenc supplies all the PVDF film used in production of the standardized shock transducer element.

Francois Bauer of ISL has developed and patented a technique of polarizing this biaxially stretched PVDF that maximizes the piezoelectric output and produces reproducible values of remnant polarization.[4,5] His process involves using a cyclic, 500 MV/m electric field to rotate the hydrogen and fluorine pairs and to dissipate local space charges.

The result of this effort was the development of a standardized PVDF shock transducer element. Figure 2-1 is a representation of the standardized element. The PVDF film is 25 μm thick biaxially stretched PVDF with gold-over-platinum sputtered electrodes. The active area is poled using the Bauer process to a remnant polarization of 9 $\mu C/cm^2$.

Characterization

As part of a cooperative effort with ISL, Sandia National Laboratory has performed a characterization study on the standardized PVDF shock element.[6] Through a large number of precision planar impact experiments, a shock response calibration relating piezoelectric charge versus stress has been produced. Equation (2-1) is Graham, et al.'s polynomial fit to the shock data where σ is stress in GPa and q is charge density in $\mu C/cm^2$.

.010 to .337 GPa:

$$\sigma = 2.86 \times 10^{-5} + 4.415 \times 10^{-1} q + 1.027 q^2 - 5.41 \times 10^{-1} q^3$$

.337 to 2.369 GPa:

$$\sigma = -5.47 \times 10^{-3} + 6.42 \times 10^{-1} q + 3.61 \times 10^{-1} q^2 - 7.49 \times 10^{-3} q^3 \qquad (2\text{-}1)$$

2.372 to 10 GPa:

$$\sigma = -7.43 \times 10^{-3} + 6.25 \times 10^{-1} q + 5.20 \times 10^{-1} q^2 - 2.31 \times 10^{-1} q^3 + 9.87 \times 10^{-2} q^4 - 1.12 \times 10^{-2} q^5$$

The results show a smooth curve from 10 MPa through 10 GPa which is independent of loading path. This curve is given in Figure 2-2. Response data above 10 GPa has been recently released, including results at pressures approaching 50 GPa.[7]

Performance Characteristics

Sensitivity. Because of its high sensitivity to changes in stress, PVDF output has a high signal-to-noise ratio, making the use of an external amplifier unnecessary. For example, underwater shock experiments are often electrically noisy because of capacitive coupling of the gauge and water, charge polarization, etc.; however, when circuitry is chosen carefully, PVDF transducers yield excellent underwater records.

Wide Pressure Band. PVDF is capable of measuring stress within a wide band of magnitudes. Pressures less than 1 MPa and greater than 10 GPa can be measured.

Short Shock Transit Time. The PVDF sensors are so thin that, for many experiments, it is virtually "invisible" to the incident shock pulse. This feature is especially true for underwater experiments where shock rise times are long.

Rate of Change of Stress. PVDF is the only stress gauge that can directly measure the time derivative of stress.

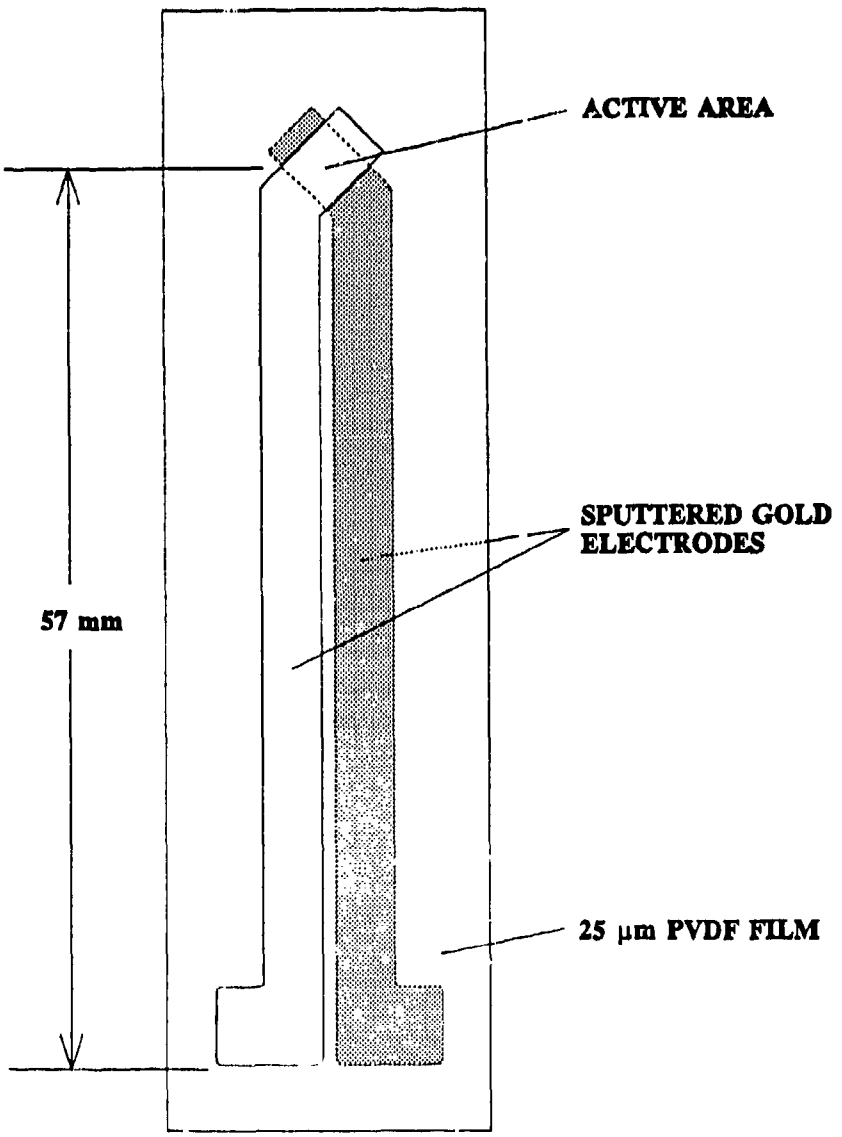

FIGURE 2-1. THE STANDARDIZED ISL/BAUER PVDF TRANSDUCER ELEMENT

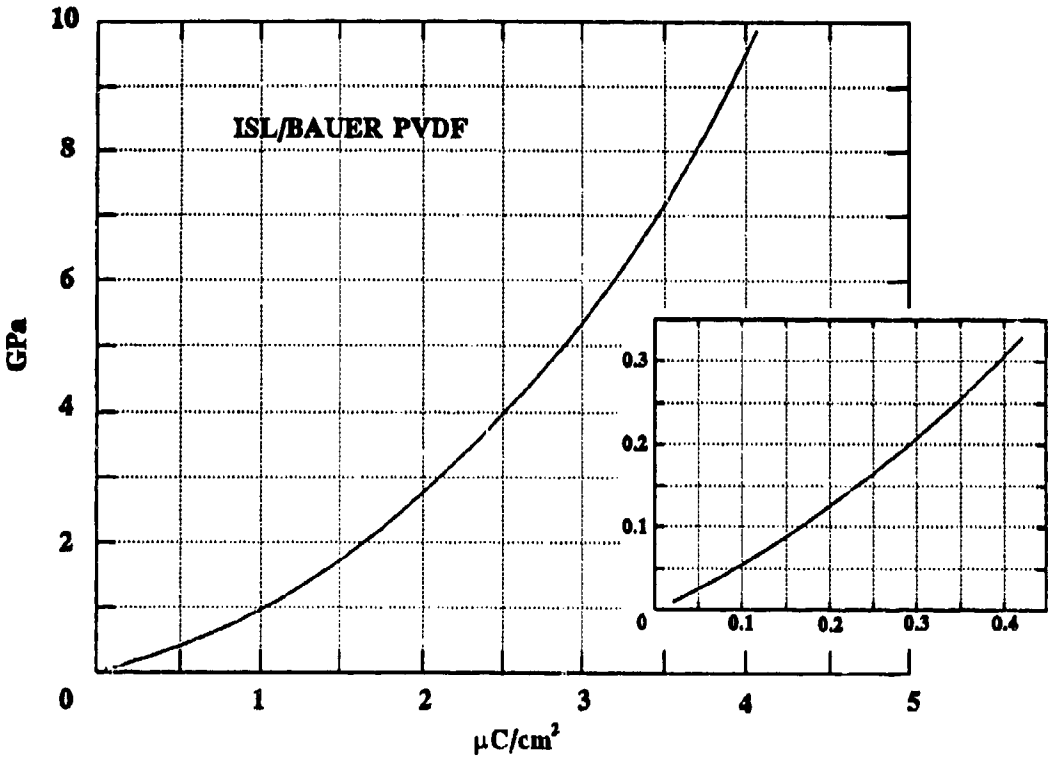

FIGURE 2-2. SHOCK RESPONSE CHARACTERIZATION DATA FOR ISL/BAUER PVDF

Potential Problems. The use of PVDF is not problem-free. In common with all stress gauges, PVDF is sensitive to lateral strains which can perturb stress-time data. However, some of our underwater work reported here suggests that these strain effects may not greatly influence peak stress measurements, though more study is needed to obtain conclusive information.

PVDF is sensitive to large thermal gradients, which can depolarize the hydrogen-fluorine pairs resulting in lower charge output and erroneous stress data. Applying thermal shields of copper, aluminum, or gold coatings has been shown to eliminate this effect.[1]

CHAPTER 3

TECHNIQUES

PVDF gauge output is sensitive to *changes* in stress, σ; i.e., the rate of change of charge output, dQ/dt, is related to the rate of change of stress, dσ/dt. The charge, Q, produced by the element is a measure of the stress in the element. At NAVSWC, two methods of operation have been employed for PVDF transducers. In one method, the charge generated by the gauge element is measured to get a direct record of the stress input to the gauge element. This mode of operation is called the charge mode and is best suited for use in experiments measuring shock pulses with long rise times. The second technique measures the *rate* of charge production, which yields data proportional to stress rate, dσ/dt. This technique is known as the current mode and is best used to measure shocks with short rise times (tenths of μs). The choice of which technique to use depends upon the desired measurement and the conditions under which the measurement is being made.

CHARGE MODE OPERATION

Circuit Design

A charge measurement is achieved by monitoring the voltage across a capacitor wired in parallel with the PVDF element as shown in Figure 3-1. The value of the capacitor, C, is adjusted to suit the experiment being performed. The work in this report used a 25 mm^2 active area sensor with a 100 nF capacitor across it and a 50 Ω resistor between the capacitor and the signal cable. The 50 Ω resistor matches the circuit to the 50 Ω impedance cable so that the capacitance of the cable can be ignored when analyzing the data. To properly use this matching technique, the circuit must be kept close to the PVDF; i.e., between the element and the cable. If the integrating circuit is attached far from the gauge, then the cable reactance must be accounted for in the corrections discussed below.

The charge mode circuit described above is, in effect, a low pass filter. If the shock pulse is a high frequency event; i.e., if it has a very short rise time, then the charge mode circuit may yield erroneous data if this frequency exceeds the bandwidth of the circuit. In our work, the rise time of our pressure pulse was fairly long, approximately 100 ns (3.5 MHz equivalent bandwidth). The capacitor value was chosen so that the resonant frequency of the circuit was well above 3.5 MHz. One benefit of the filtering is that high frequency noise is smoothed out. This effect is desirable in high noise environments such as underwater field tests.

Data Reduction

When the element is stressed, charge is generated on the two electrodes. The change in charge, dQ/dt, becomes the current, i_c, flowing to the capacitor, C, in

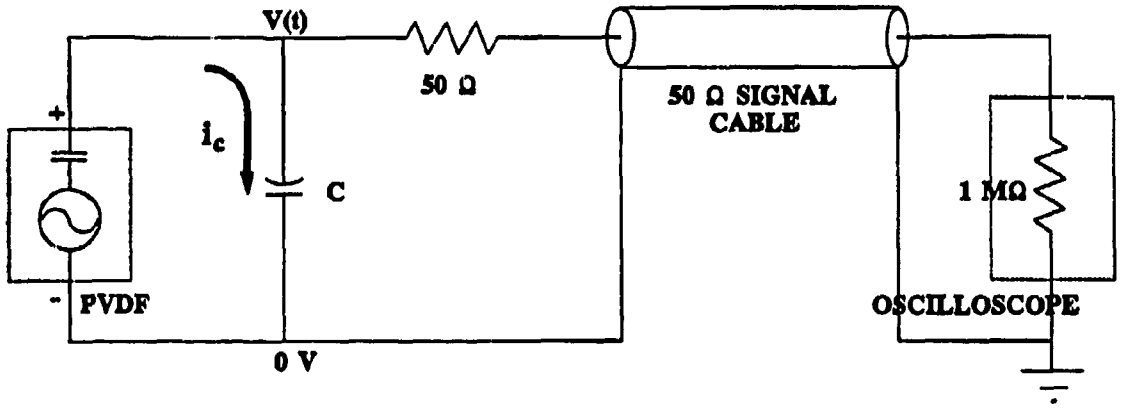

FIGURE 3-1. PVDF TRANSDUCER IN A CHARGE MODE CIRCUIT

Figure 3-1. As the capacitor is charged, the oscilloscope monitors the voltage across it. This measured voltage is representative of the charge produced by the PVDF. Since the charge produced is a measure of the stress on the PVDF element, Equation (2-1), then the voltage-time record from a charge mode transducer is representative of the stress-time profile.

The charge on the capacitor is related to the measured voltage by

$$Q(t) = C \times V(t) \tag{3-1}$$

where Q is the charge in Coulombs, C is the capacitance in Farads, and V is the voltage in volts. In order to apply Equation (2-1) to obtain stress in GPa, the charge must be expressed in units of $\mu C/cm^2$. Simple arithmetic gives:

$$q(t) = \frac{C \times V(t)}{A} \times 10^{-6} \tag{3-2}$$

where q is the charge density in $\mu C/cm^2$ if the area A of the PVDF element is in cm^2. This charge density is then used in Equation (2-1) to calculate the stress in the PVDF.

Signal Prediction

In order to properly set oscilloscope voltage sensitivities, it is necessary to have some knowledge of the peak signal that is expected. For experiments using charge mode PVDF transducers, signal estimates are made by using a prediction of the peak stress magnitude. Substituting this value into the stress-charge calibration, Equation (2-1), the expected peak charge output from the PVDF can be calculated. Knowing the charge mode circuit parameters and solving Equation (3-2) for V(t), an estimate of the peak voltage record can be made. If desired, the value of the shunt capacitor, C, can then be changed to adjust the circuit output to suit experimenter preference. This method makes setting oscilloscope sensitivities simple in experiments where only rough estimates of peak pressure are available.

"Direct" Stress Measurement

Since the signal output from the transducer is a function of the stress input, the scope record is a fair representation of the structure of the stress profile even before performing data analysis. Any obvious deviation from the expected pulse structure can be seen immediately.

CURRENT MODE OPERATION

Circuit Design

The current mode technique takes full advantage of the stress rate sensitivity of PVDF. A small resistor, r, is attached in parallel with the PVDF element as shown in Figure 3-2. The current through the resistor is measured. Since the current is defined as the rate of change of charge, dQ/dt, and the charge output Q is a function of gauge stress σ, the output from a current mode PVDF transducer is a measure of

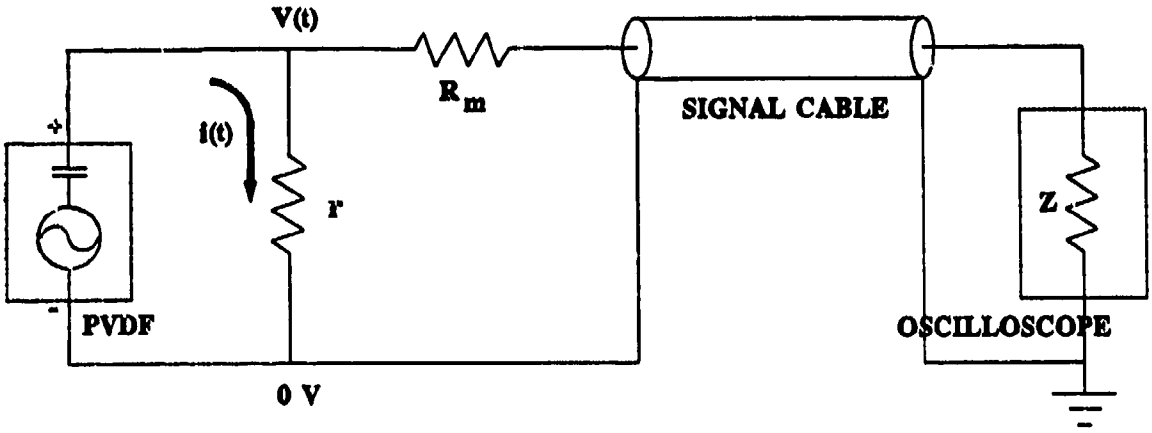

FIGURE 3-2. PVDF TRANSDUCER IN A CURRENT MODE CIRCUIT

stress rate, dσ/dt. To obtain a stress measurement, the data must then be numerically integrated. Since the output from current mode PVDF transducers represents the rate of change of stress during a shock pulse, they are very sensitive to the structure of the shock profile.

Data Reduction

The oscilloscope measures the voltage V(t) across the shunt resistor, which is related to the current i(t) by Ohm's Law. For the circuit shown in Figure 3-2, analysis yields:

$$V(t) = i(t) \frac{r(R_m + Z)}{r + R_m + Z} x \frac{Z}{R_m + Z}$$

which simplifies to:

$$V(t) = i(t) \frac{rZ}{r + R_m + Z} \tag{3-3}$$

where r is the shunt resistance, R_m is the matching resistor, and Z is the input impedance of the oscilloscope.

Substituting:

$$i(t) = \frac{dQ(t)}{dt}$$

into Equation (3-3), and solving for dQ(t) gives:

$$dQ(t) = \frac{r + R_m + Z}{rZ} V(t)\, dt \tag{3-4}$$

Integrating Equation (3-4) and dividing by the active area, A, in cm^2, gives the charge density:

$$q(t) = \frac{r + R_m + Z}{rZA} \int V(t)\, dt \tag{3-5}$$

which is then substituted into Equation (2-1) to obtain stress.

In our work, the shunt was typically 1 to 3 Ω, with R_m = 50 Ω to match the transducer circuit to the 50 Ω coaxial cable and the 50 Ω oscilloscope impedance.

Signal Prediction

To predict the peak voltage magnitude at the oscilloscope, estimates of the pulse rise time, τ, and of the peak stress are necessary. Recall that:

$$i(t) = \frac{dQ(t)}{dt}$$

Assuming a steady rate of change of charge during the pulse rise, the PVDF element produces a quantity of charge, Q, so therefore the current through the shunt resistance is:

$$i \approx \frac{Q}{\tau} \tag{3-6}$$

Furthermore, we know that the charge density is the charge per unit of area, or:

$$q \approx \frac{Q}{A}$$

A value for q is obtained from the calibration data, Equation (2- 1).

Returning to Equation (3-3) and substituting the above, we obtain an expression for estimating oscilloscope voltage as a function of pulse rise time, peak charge, and circuit parameters:

$$V_{peak} = \frac{qA}{\tau} x \frac{rZ}{r + R_m + Z}$$

Digitizer Sensitivity. Care must be taken when using digitizing equipment in an experiment using PVDF in the current mode. If the current mode PVDF output is recorded at a low digitizer sensitivity, the data can be distorted. At low sensitivities there is a greater voltage step between each of the levels in the analog-to-digital (A/D) converter of the digitizers compared to the incoming peak voltage. Therefore, it takes a larger voltage change in the incoming data to effect a change of one voltage step in the digitizer. Gradual rises or falls in the data can become stair steps as the digitizer jumps from voltage level to voltage level. Also, small voltage changes in the incoming data may not even be recorded if they are not large enough to initiate a change between levels. Because of the large voltage steps, relatively small signal changes can result in erroneous data if the digitizer was at the threshold between two voltage levels. Figure 3-3 demonstrates some of these problems. The integrated records shown here are signals from the same PVDF gauge operating in the current mode. Note how the lower sensitivity record ($\pm$20 V) lacks the structure following the peak shown in the higher sensitivity trace ($\pm$4 V).

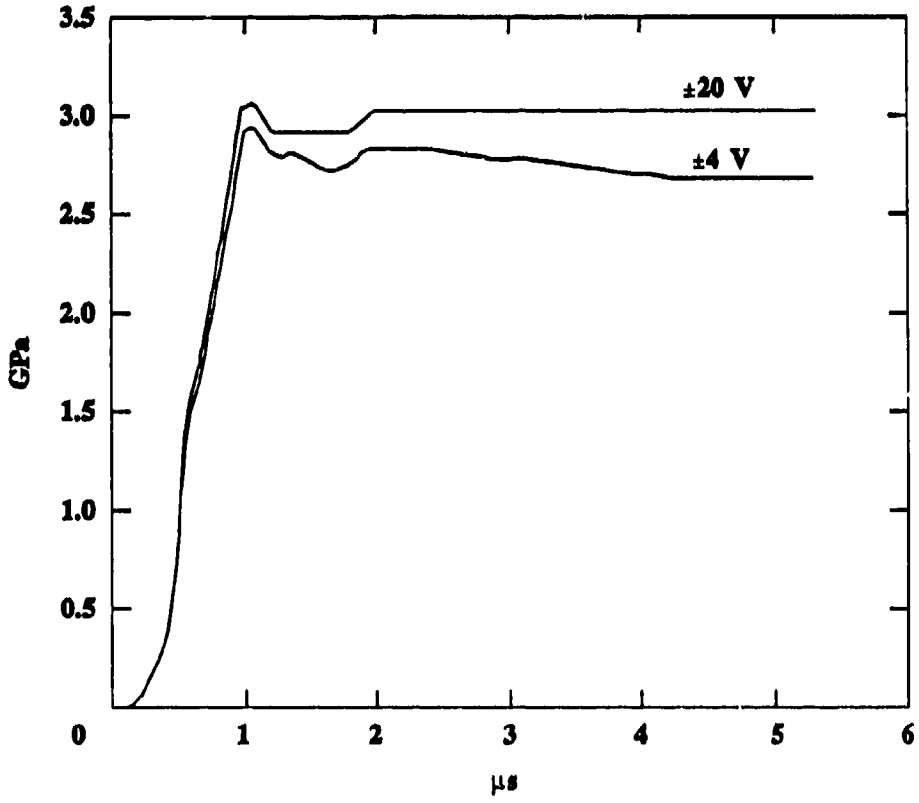

FIGURE 3-3. ERROR IN CURRENT MODE DATA CAUSED BY LOW DIGITIZER SENSITIVITY

CHAPTER 4

EXPERIMENTAL APPLICATIONS OF PVDF SHOCK TRANSDUCERS

This chapter will describe several experiments performed at NAVSWC, White Oak. General descriptions of the experimental arrangements will be given, followed by a brief discussion of the results. Chapter 5 will cover the results in more detail.

STRESS MEASUREMENTS AT A WATER/SOLID INTERFACE

The shock conditions at the interface of two materials of different shock impedance; e.g., at a fluid/solid interface, give rise to measurement difficulties. PVDF pressure transducers mounted on the solid surface are exposed to nonuniaxial stress and strain, including such effects as radial expansion. Earlier work has demonstrated that the PVDF polymer response is affected by radial expansion, yielding erroneous stress data.[8] In an effort to quantify and minimize these effects, we have performed preliminary work to study the response of a surface-mounted PVDF transducer subjected to underwater shocks.

A tandem PVDF transducer configuration, consisting of two PVDF gauges mounted to either side of a thin plate, was studied in underwater shock wave experiments.[9] In this arrangement, one transducer element produces charge due to both the stress and the strain in the plate. The other gauge is positioned such that its response is essentially due only to the strain in the gauge. The signals from each transducer are compared to obtain the stress, assuming the strain effects are adequately handled by this approach. A numerical approach is used to minimize the effect of circuit inconsistencies.

Experimental Arrangement

Water Gap Arrangement. The experiment used a water shock attenuator, or gap, arrangement to deliver a shock of prescribed magnitude to a target plate. This gap arrangement, shown in Figure 4-1, has been adapted from one used at the Naval Weapons Center (NWC), China Lake, and has been pressure-distance calibrated at NAVSWC.[10,11] The calibration is given in Figure 4-2.

An explosive donor, a 50.8 mm x 50.8 mm cylindrical Pentolite (50/50 PETN/TNT) charge, was detonated underwater at 50 mm from the target. The calibration gave the pressure in the water before the shock entered the plate and a simple impedance mismatch calculation was performed to estimate the input stress to the target.

Target/Aquarium Assembly. Two PVDF elements were bonded to either side of a 150 mm diameter target plate with a 10:3 mixture of Dow Epoxy Resin 332 and Dexter-Hysol hardener 3561. At room temperature, this mixture has a very low

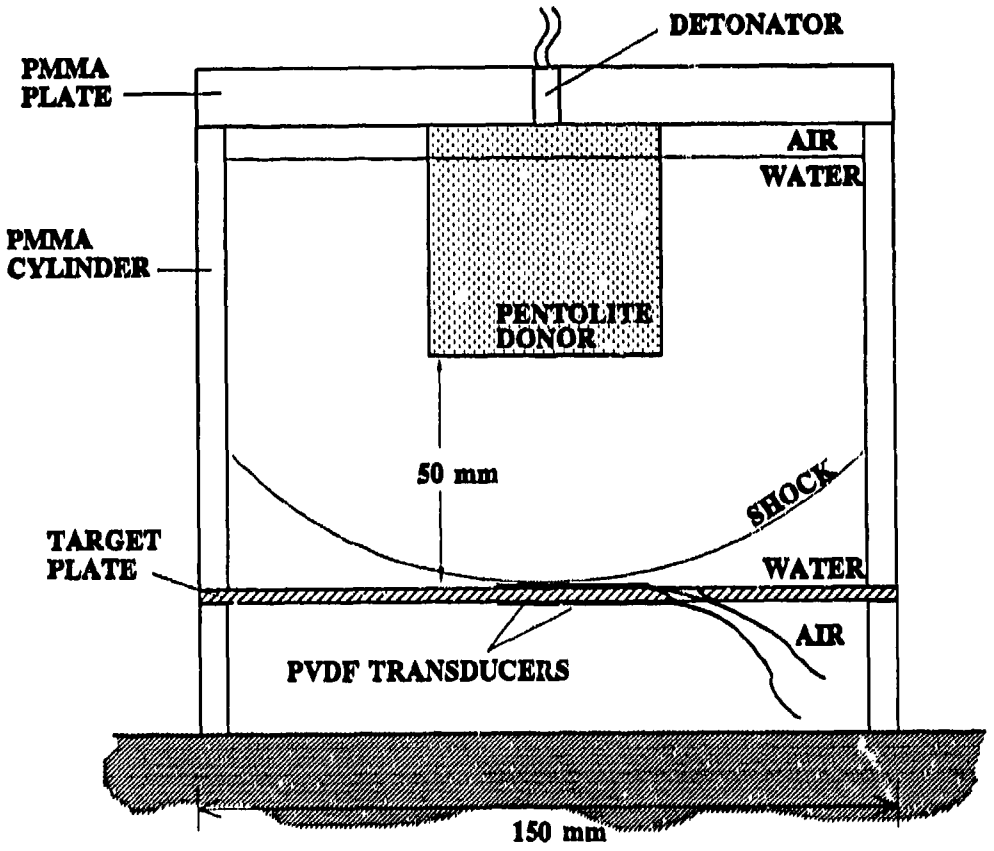

FIGURE 4-1. EXPERIMENTAL ARRANGEMENT TO MEASURE STRESS AT A WATER/SOLID INTERFACE

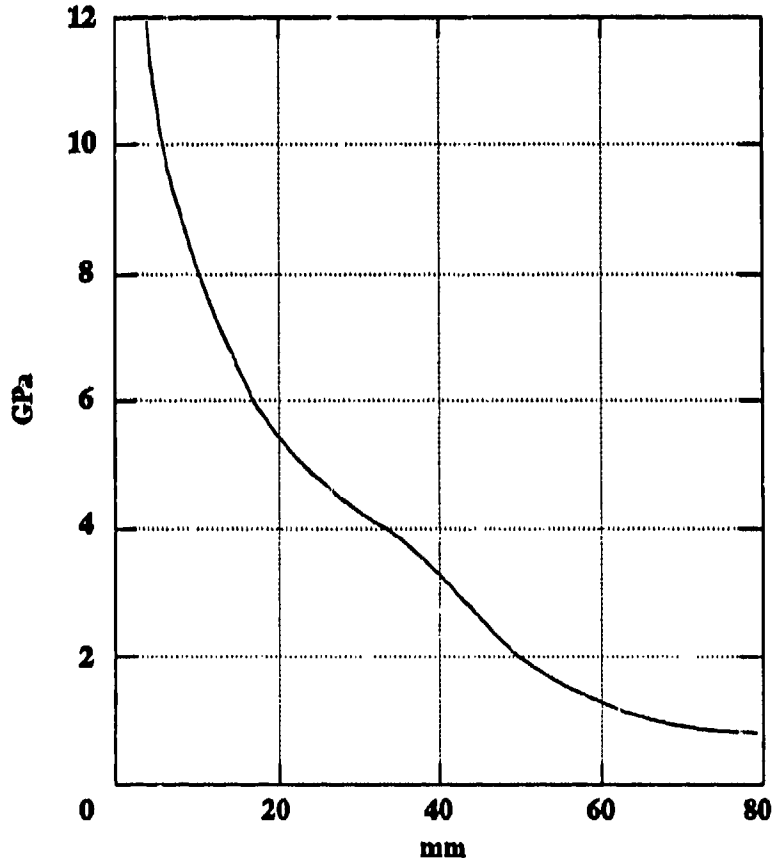

FIGURE 4-2. PRESSURE-DISTANCE CALIBRATION OF A CYLINDRICAL PENTOLITE DONOR IN WATER

viscosity, and with light pressure applied, a bond thickness on the order of 3 μm can be obtained. The plate material was 6.35 mm thick PMMA. A 140 mm inner diameter PMMA cylinder bonded to the plate with silicone rubber served as an aquarium. A thin film of mylar was applied over the top transducer to form a watertight seal. The cylinder was filled with fresh water.

Transducer Configuration. The PVDF shock transducer was composed of two 25 mm^2 PVDF shock transducer elements in a tandem arrangement composed. The first transducer element was placed at the water/plate interface. The second transducer element was positioned on the opposite side at the plate/air interface. The idea was to obtain a record of a combination of stress and nonaxial strain from the first transducer element and a record of the nonaxial strain effects alone from the second PVDF element. The stress at the plate/air interface cancels on reflection, so data from a transducer mounted here is representative of the nonaxial strain in the plate with no stress contribution after a few reverberations in the gauge as long as the gauge remains against the plate. Since PVDF has a shock impedance slightly higher than that of PMMA, the plate/transducer junction remains intact during the experiment.

The PVDF transducers were used in the charge mode circuit shown schematically in Figure 3-1. The details of the circuit assembly are given Figure 4-3. The 100 nF capacitor was soldered to a short length of flexible circuit board which was then attached to the gauge element through two small copper tabs soldered to the PVDF with low temperature indium-bismuth solder.

Recall that the charge produced is proportional to the stress input to the transducer according to Equation (2-1). For this work, the stress input σ was easier to predict than the stress rise time. With the peak stress approximately known, the signal peaks were more accurately estimated, which simplified setting oscilloscope sensitivities. The stress rise time, though not exactly known, was expected to be on the order of 100 ns, so the fast response of the current mode was not needed. Also, wide band electrical noise can be generated due to shock induced polarization of the water, and transducers are more susceptible to this noise in current mode as opposed to charge mode. For these reasons, the charge mode configuration was chosen over the current mode.

Output Estimates. When detonated, the Pentolite donor introduces an approximately 11 GPa shock to the water. After traveling the 50 mm to the plate, the shock decays to a peak pressure of 2.1 GPa in the water. As the shock enters the plate, the pressure rises due to the impedance mismatch. Figure 4-4 is a plot of the Hugoniots for water, PMMA, and aluminum, and demonstrates the graphical technique for performing an impedance mismatch calculation where shock attenuation is ignored. The aluminum Hugoniot is shown because some shots were performed with a 3.17 mm thick 6061-T6 aluminum plate in place of the PMMA. A 2.5 GPa peak was predicted for the PMMA and 4.3 GPa for the aluminum. These stress values were verified with computer code calculations. Applying Equation (2-1) to these stress values yielded charge estimates, which were used to calculate output voltages.

Results

PMMA Plate. The results of one experiment are shown in Figure 4-5. After data reduction, the measured peak stress at the water/PMMA interface agrees with

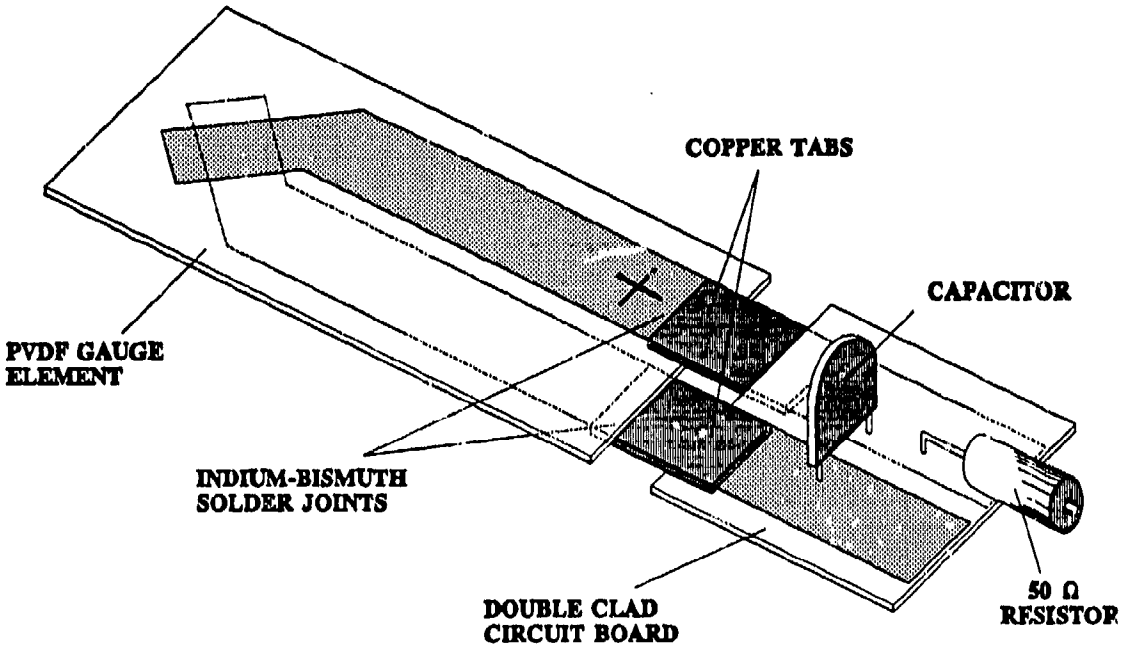

FIGURE 4-3. PVDF TRANSDUCER CIRCUIT PACKAGING

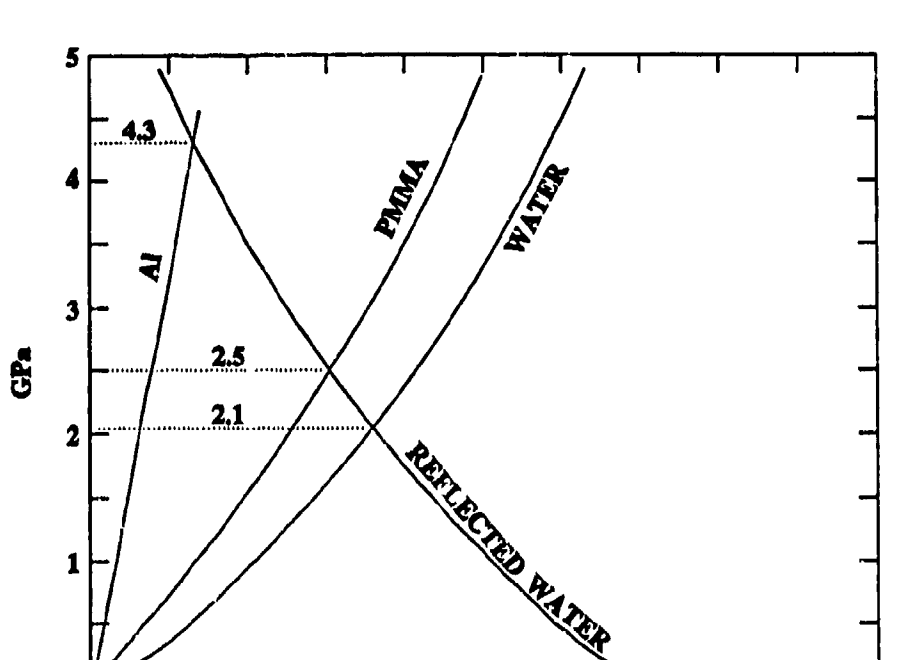

FIGURE 4-4. GRAPHICAL IMPEDANCE MISMATCH CALCULATION

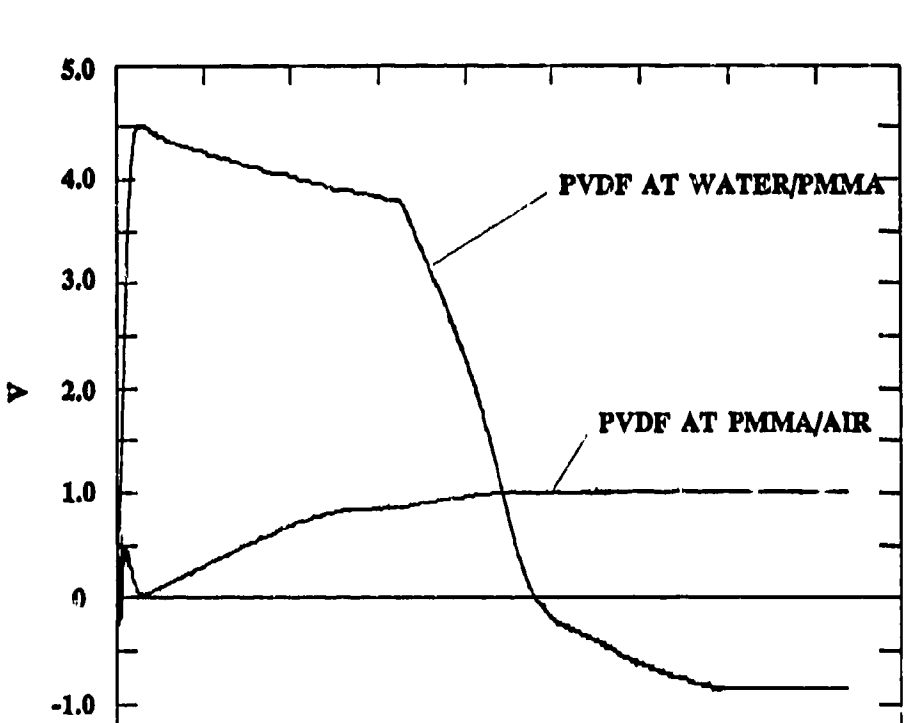

FIGURE 4-5. SIGNAL FROM PVDF AT THE WATER/PMMA INTERFACE

the predicted value of 2.5 GPa. At about 3 μs the rarefaction arrives from the PMMA/air interface and interferes with the input pulse measurement. The calculated reflected stress in the PMMA due to the water/PMMA interface was approximately 100 MPa. However, the signal measured is negative, possibly due to a combination of strain effects and shock decay.

The record from the transducer at the PMMA/air interface shows a different structure. The initial ringing in the trace may be shock-induced electrical noise generated by the PMMA. It is present for over 200 ns which is too long to be shock ring-up of the PVDF alone. The ringing is followed by a slow rise to an approximately 1 V plateau which is stable for the remainder of the record. Since the PVDF is closely matched to the PMMA, spalling of the transducer element from the plate does not occur. Therefore, this record is a result of nonaxial strain in the plate.

Aluminum Plate. Figure 4-6 shows data recorded from a transducer at the water/aluminum interface. After data reduction the stress record was obtained. It is plotted with a record from another experiment in Figure 4-7. The agreement between the two records is excellent. Both records show peaks near the predicted 4.3 GPa with rise times of 110 to 120 ns. The shock "ring-up" of the transducer package is evident on the leading edge of the records and was complete in approximately 40 ns.

The peak is followed by a stepped decay. The steps occur at approximately 1.1 μs intervals, which is twice the shock transit time through the 3 mm plate. Each step is the arrival of a reflected pulse from the aluminum/air interface.

A gauge mounted at the aluminum/air interface would have spalled off almost immediately upon shock arrival because of PVDF's lower shock impedance. Therefore, no results could be obtained for nonaxial strain of the aluminum plate.

IMPULSE MEASUREMENT OF PBXW-123

An experiment was performed to measure the impulse at the end of a reacting cylinder of explosive using both PVDF and manganin pressure gauges. This instrumentation was added to an experiment involving a streak camera measurement of the detonation velocity of a cylindrical charge of PBXW-123. PBXW-123 is an underwater explosive with a large failure diameter. The PVDF gauge records show that the charge did not detonate. This experiment represents our first attempt to measure stress in a reacting explosive with PVDF gauges. Although the explosive itself failed to perform in this configuration, the PVDF transducers obtained useful data. One goal of this experiment was to compare the PVDF stress records obtained with the charge and current mode methods.

Experimental Arrangement

General. As an addition to a PBXW-123 detonation velocity measurement experiment, an instrumented Teflon® gauge block was attached to the end of the charge. Teflon was chosen because it has a shock impedance which closely matches that of the explosive.

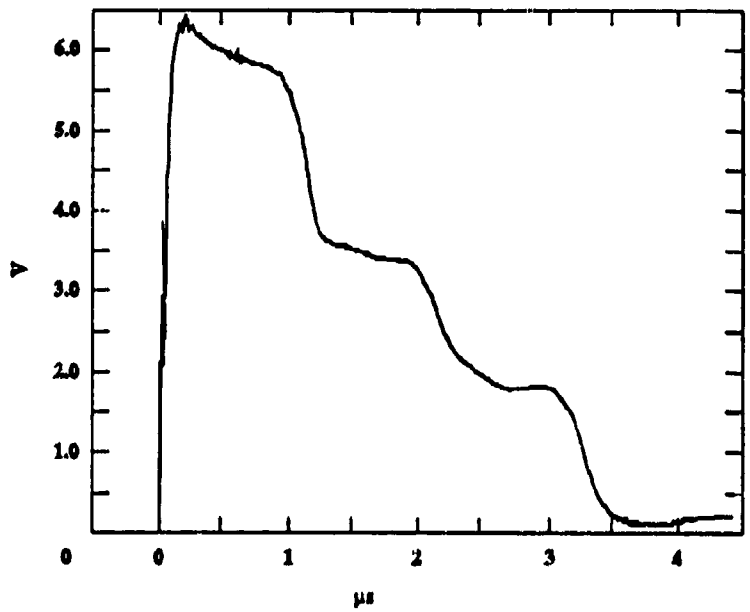

FIGURE 4-6. SIGNAL FROM THE PVDF TRANSDUCER AT THE WATER/ALUMINUM INTERFACE

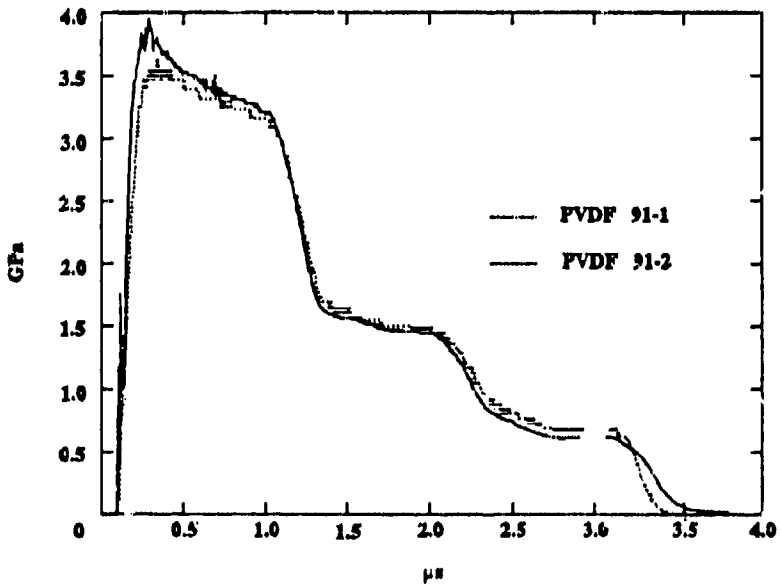

FIGURE 4-7. STRESS AT THE WATER/ALUMINUM INTERFACE

Two 25μm thick, 5 mm x 5 mm active area PVDF transducer elements were epoxied to the Teflon. A Dynasen* gauge package consisting of one manganin gauge sandwiched between thin sheets of Teflon was epoxied in front of the PVDF gauges. The manganin gauge was positioned so that shock reflections from the manganin did not affect the PVDF records. The PVDF elements were each approximately 8 mm off center. The block was then mounted to the end of a 12.5 cm diameter, 50 cm long PBXW-123 using silicone vacuum grease between the surfaces to eliminate any air gaps. A bead of silicon RTV around the outside of the interface secured the block to the charge, and the whole assembly was supported in a cradle. This arrangement is schematically shown in Figure 4-8.

Transducer Configuration. One transducer was operated in the charge mode; the second gauge was used in the current mode. The circuits used for the transducers were the same as those discussed in Chapter 3. The charge mode gauge used a 100 nF shunt capacitor, and the current mode gauge used a 3 Ω shunt resistor. The record from the current mode gauge was numerically integrated to obtain stress.

Output Estimates. A 12 to 15 GPa peak stress with an approximately 100 ns rise time was estimated if the explosive detonated. Using the methods outlined in Chapter 3, peak output estimates were made, giving a peak of approximately 10 V from the charge mode gauge and 14 V for the current mode gauge.

Results

As mentioned above, the explosive failed to detonate. However, the PVDF transducers and manganin gauge produced stress data. The records from the PVDF transducers are shown in Figure 4-9. Recall that the current mode gauge output is a measure of stress rate over time; thus, the peaks and valleys reflect changes in slope in the stress-time record.

It is important to note here that these records have been time-shifted to appear coincident so that direct comparison is easier. The current mode record actually began 200 ns after the charge mode record, probably due to large wave curvature in the PBXW-123. (High wave curvature was measured in an experiment with a 10.2 cm diameter charge.) Also, the gauges were not positioned in the exact same place.

After the appropriate corrections, (e.g., scaling, necessary integration, application of the stress calibration), the stress records were obtained. The results are given in Figure 4-10 along with the manganin gauge data. The charge mode record gives a peak stress of 3.0 GPa which decays to 2.6 GPa after about 3 μs and then remains stable. The integrated current mode data shows a 2.5 GPa peak followed by a decay to 2.3 GPa. The manganin gauge record shows a peak stress of 2.8 GPa. These low stress magnitudes certainly indicate an absence of detonation. The long sustained plateau starting at about 2.5 μs is probably due to gauge stretching and relief wave arrival. These effects were expected to occur after a few microseconds.

This experiment represents our first attempt to use PVDF pressure transducers to measure the stress-time profile in a reacting Navy explosive. Though the experiment was not designed to measure pressure in a failing detonation wave, the

*Dynasen, Inc., 20 Arnold Place, Goleta, CA 93117.

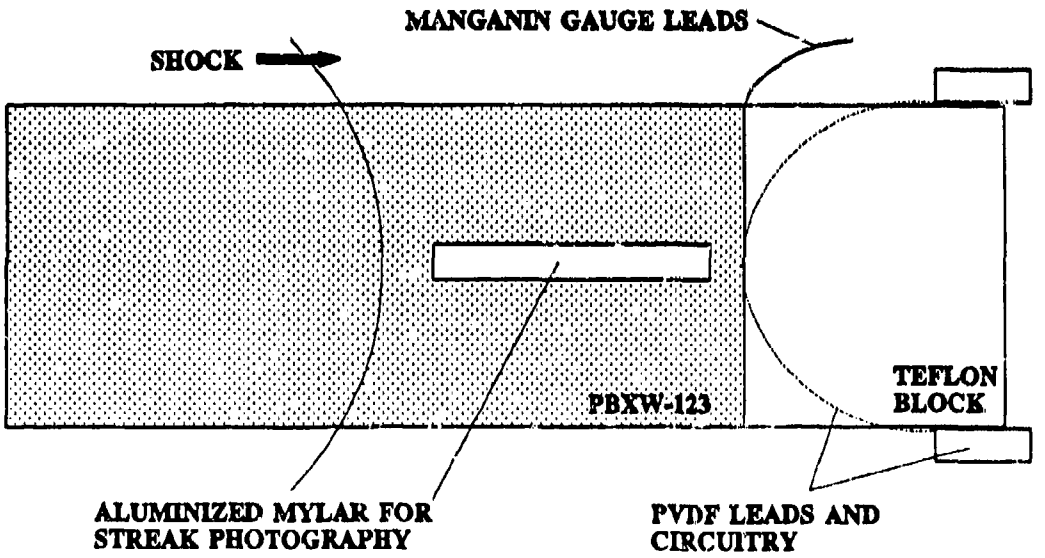

FIGURE 4-8. EXPERIMENTAL ARRANGEMENT TO MEASURE THE IMPULSE FROM A REACTING CYLINDER OF PBXW-123

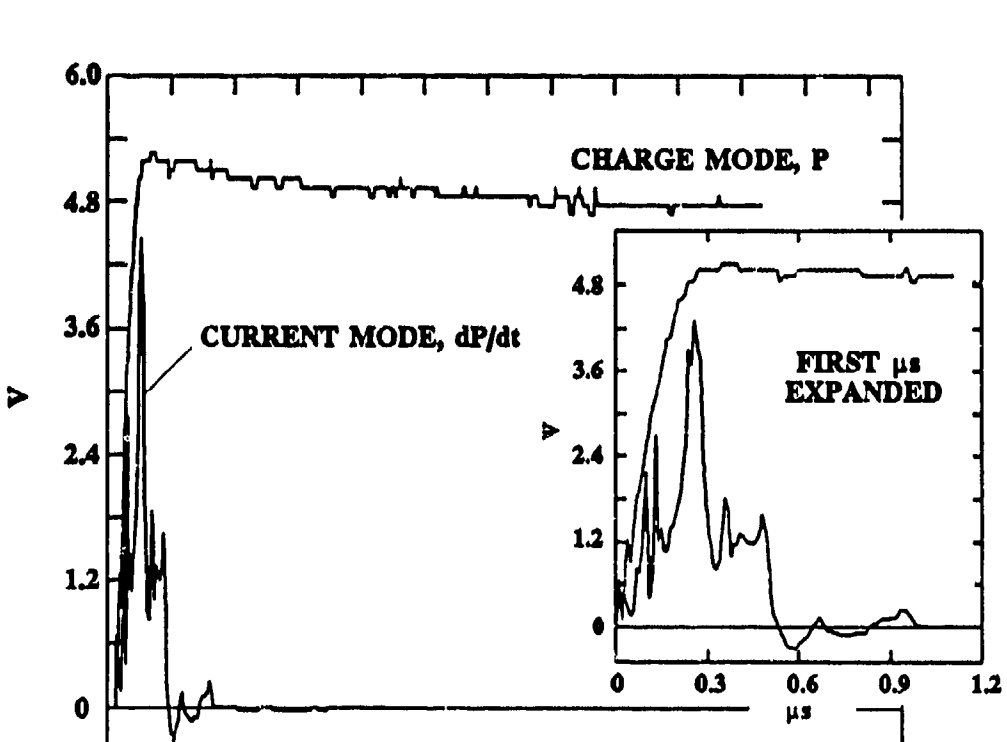

FIGURE 4-9. CHARGE MODE AND CURRENT MODE RECORDS FOR THE PBXW-123 IMPULSE EXPERIMENT

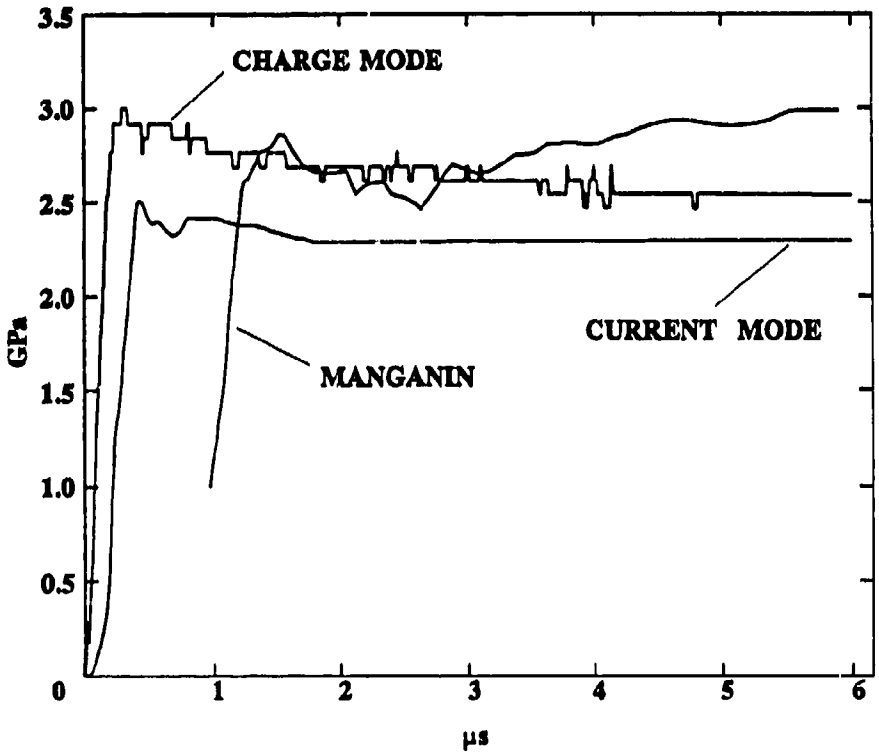

FIGURE 4-10. STRESS IN A REACTING CYLINDER OF PBXW-123 AT THREE ADJACENT GAUGE LOCATIONS

PVDF transducers did produce useful data. The agreement of the two PVDF records and the PVDF data with the manganin gauge data is good.

FLYER PLATE PERFORMANCE EVALUATION

An explosively driven aluminum flyer plate was designed for use as a shock input device for a series of experiments. The system was designed to yield flyer velocities above 2.5 mm/μs. A potential problem with an explosively driven flyer plate is that it may split into thin plane layers (i.e., spall). Multiple plates impacting the target will result in a multi-peaked shock instead of the desired flat top shock. Our explosively driven flyer design is shown in Figure 4-11 and is similar to that used by Erkman in his work on shock wave attenuation in aluminum.[12] Erkman showed that a thin layer of Detasheet® explosive placed between the metal driver plate and the metal flyer plate reduced spalling of the flyer plate. However, a plane one-dimensional hydrocode calculation showed that our design would spall.[13] However, the equations of state for Detasheet and the driver explosive (PBXN-110) were not accurately known, resulting in uncertainty in the calculation's prediction of spall. In order to evaluate its performance, a PMMA target plate was instrumented with PVDF transducers and was struck with the flyer. The stress data obtained shows that the aluminum flyer spalled into at least two pieces, giving a double impact.

Experimental Arrangement

General. Figure 4-11 gives the details of the experimental assembly. A 25 mm^2 PVDF gauge was mounted to the surface of a 12.7 mm PMMA plate to measure the induced stress in the PMMA by a 6 mm thick 6061-T6 aluminum flyer plate. The flyer was explosively driven using a combination plane wave booster/explosive charge assembly.

Transducer Configuration. The PVDF element was used in the charge mode with a 100 nF capacitor shunt as shown in Figure 3-1.

Output Estimates. A flyer velocity of approximately 2 to 4 mm/μs was expected from the configuration shown. This velocity was expected to result in an induced stress loading on the front face of the PMMA of approximately 10 to 20 GPa. The rarefaction from the back surface of the plate was expected to arrive after about 2 μs. If the aluminum flyer plate spalled, the result would be a multiple impact of flyer material on the PMMA, though the peak stress magnitude would remain about the same.

Results. The record, converted to stress using Equation (2-1), is shown in Figure 4-12. The initial slow-rise ramp is due to the air shock ahead of the flyer (the chamber was evacuated only to about 40 microns). The double hump structure confirms that the flyer did indeed spall. The 9.8 GPa peak stress gives a calculated flyer velocity of 3.1 mm/μs. The 1.75 μs time separation between impacts suggests that the layers were separated by less than 5.4 mm. Based on the 1.5 μs width of the first pulse, the first layer was approximately 2 mm thick.

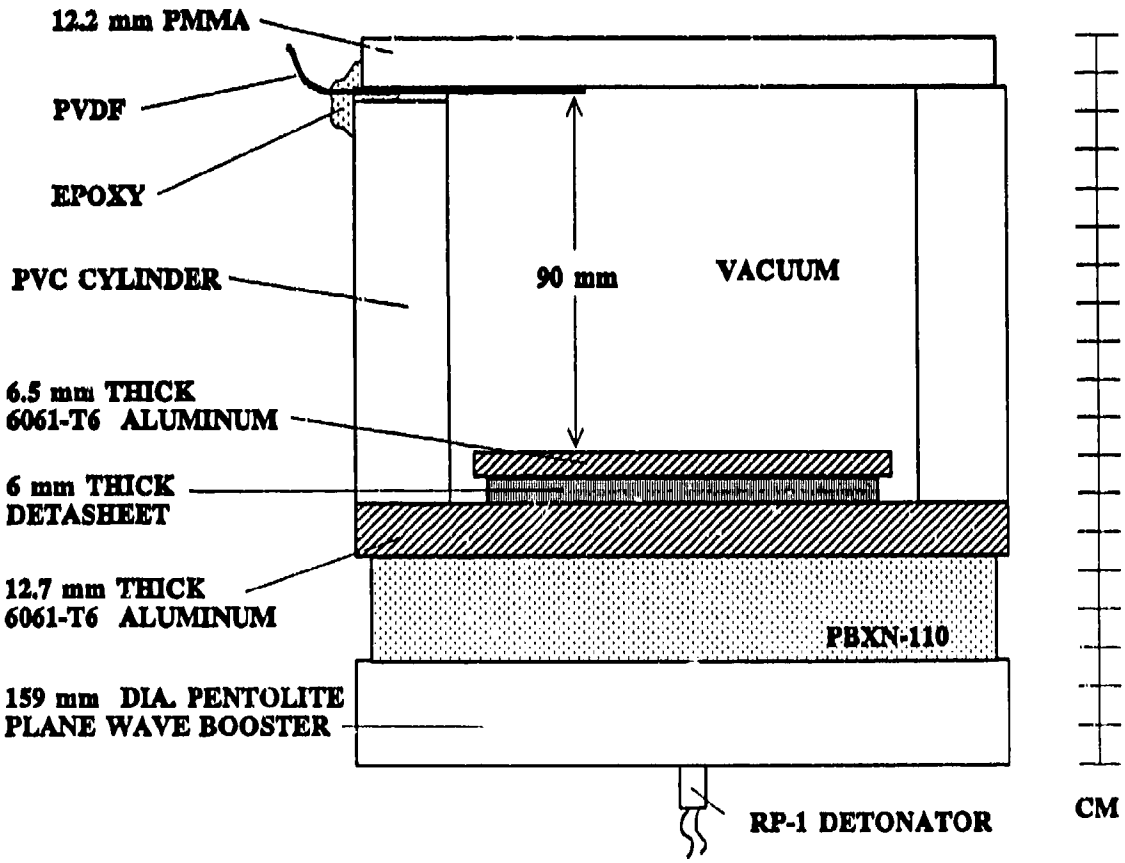

FIGURE 4-11. FLYER PLATE PERFORMANCE EXPERIMENTAL ARRANGEMENT

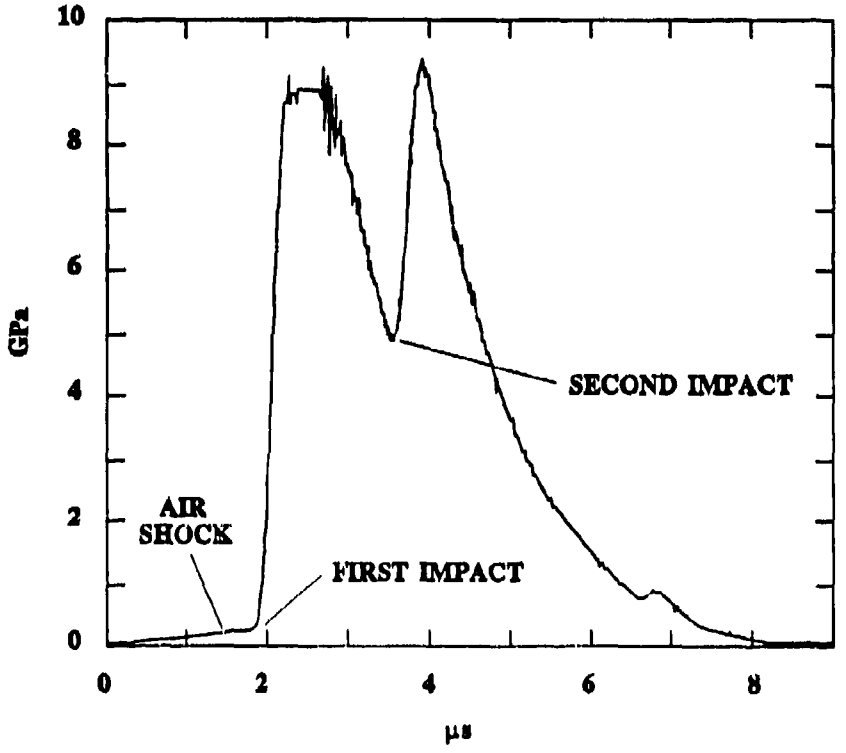

FIGURE 4-12. DOUBLE IMPACT FROM A SPALLING ALUMINUM FLYER PLATE

CHAPTER 5

DISCUSSION AND CONCLUSIONS

The PVDF stress gauge has allowed the measurement of shock wave response of several materials under moderate to high stress. It can be used to measure the shock pulse in water close to detonating explosive charges. In this stress range, greater than 6 kbar in water, standard crystal gauges such as tourmaline and lithium niobate cannot survive or give reliable results. For stress pulses with long rise times, the PVDF gauge used in the charge mode is simple to use and yields accurate results. For special applications with very fast shock wave rise times, the PVDF can be used in the current mode, which will give data representing the time derivative of stress. It is the only stress gauge capable of measuring both stress and rate of change of stress.

DISCUSSION

Chapter 4 described three experimental applications performed at NAVSWC and introduced the results. This chapter will discuss the results in more detail.

Peak Stress Measurements

The three experiments described in Chapter 4 have given results close to the calculated peak stress data to within 3 percent; i.e., within the accuracy of the PVDF calibration (Equation (2-1)). The experiment measuring stress at a water/solid interface shows that peak pressure measurements do not appear to be affected by the presence of strain. Stretching of the gauge due to bowing of the PMMA plate occurs after the front of the shock wave travels past the gauge. Late-time structure is perturbed by gauge strain.

The peak stress measured in the PBXW-123 impulse experiment shows that PVDF used in both charge mode and current mode yields well correlated results. The general structure of the waveforms is the same. The difference in magnitudes is probably due to the large, asymmetric wave curvature, and non-steady state conditions. Recall that the two transducers were spaced approximately 1.6 cm from one another and that the two signals arrived 200 ns apart.

The one-dimensional flyer plate experiment yielded peak stress measurements that agreed with hydrocode calculations.[13]

Structured Shock Loading

Both the water/solid interface and the flyer plate experiments demonstrate the ability of PVDF to measure structured shock loading. In both experiments, the charge mode transducers performed well and yielded clean data.

Strain Effects

The water/solid interface experiments were performed to address the problem of the strain-induced output of PVDF. After the initial compressive shock; i.e., after the peak stress loading, the radial expansion, etc., of the PVDF element must perturb the data. The PMMA plate experiment has shown that this problem is not completely understood.

A graphical analysis was performed to estimate the stress magnitude at the water/PMMA interface after the arrival of the rarefaction from the back surface of the plate. Since water and PMMA are not exactly impedance matched, and the initial explosive shock is not flat-topped, the stress at the water/plate interface should go to some finite value upon the arrival of the first reflection from the back face. Subsequent "ringing" of reflections should eventually bring the stress level to zero. As a first order estimate, a value of around 100 to 150 MPa was determined for stress at the interface after the first reflection.

Recall that the shot record (Figure 4-5) shows the stress at the water/plate interface to go negative after one reflection. No ringing of reflections is apparent. These deviations from expected one-dimensional stress-time behavior may be the result of nonaxial strain of the gauge element. In an attempt to compensate for the strain component, the data from the two transducers were added together. When this "corrected" voltage-time profile is converted to stress, the stress after arrival of the first reflection was 8 MPa.

Perhaps another reason for the difference in the calculated result and the measured result is that the PVDF output may deviate from the charge-stress relationship (Equation (2-1)) upon unloading. The possibility of this effect was noted in previous work done at Sandia.[14]

A more thorough analysis is needed to reconcile this difference between the calculated and measured stress. First, complete modeling of the experiment is required in order to obtain an accurate stress prediction. Second, future work will incorporate strain gauge instrumentation for simultaneous stress/strain measurements.

CONCLUSIONS

It has been shown that accurate peak stress measurements can be made at the water/solid interfaces using PVDF pressure transducers. The experiments described above have shown that, using controlled techniques, PVDF gauge circuits will yield accurate, predictable results for peak stresses.

In these experiments more than just peak stress information was obtained. For example, in the flyer plate experiment, the record shows a double impact from a spalled aluminum flyer plate. The water/solid interface experiment data showed the

stair-step relief of a shock-loaded aluminum plate. The data recorded in these experiments demonstrate the versatility of the PVDF polymer in making high pressure shock measurements. Calibration of PVDF in release states will provide accurate wave profiles in future work.

Excellent results have been obtained with both the charge mode gauge circuit and the current mode gauge circuit. The charge mode gauge circuit used in this work has been proven to be a means of obtaining clean data in the underwater experiments described above. Future work will be done to evaluate current mode transducer performance in underwater applications.

FUTURE WORK

The PVDF gauge is being packaged to measure free field stress in water close to a detonating explosive charge. Stresses above 0.6 GPa in water will be measured to give data on close-in shock pulses that conventional underwater crystal gauges (such as tourmaline and lithium niobate) cannot measure. These conventional crystal gauges do not give reliable results for stresses in water greater than about .6 GPa. The crystal elements have a high shock impedance relative to water, so a shock greater than .6 GPa in water induces stresses in the crystals that exceed their elastic yield point. Also, at lower pressures, the stress data rings as shocks and reliefs reverberate inside the crystal until the stress in the crystal reaches equilibrium with the stress in the water. This ring-up process lengthens the response time of these gauges. PVDF gauge elements have a shock impedance fairly close to that of water and are thin, so shock ring-up and reverberation are not problems.

More work is needed to characterize PVDF response to strain and how to eliminate it from stress data. Also, investigation of the response of PVDF to unloading is necessary.

REFERENCES

1. *PVDF Shock Sensor Proceedings*, 11-13 Dec 1990, Sandia National Laboratory, pp. 219-224.

2. Fogelson, D. J.; Lee, L. M.; Gilbert, D. W.; Conley, W. R.; Graham, R. A.; Reed, R.P.; and Bauer, F., "Fabrication of Standardized Piezoelectric Polymer Shock Gauges by the Bauer Method," *Shock Waves In Condensed Matter 1987*, Elsevier Science Publishers, B.V., 1988, pp. 615-618.

3. Bauer, F., "Behavior of Ferroelectric Ceramics and PVF_2 Polymers Under Shock Loading," *Shock Waves in Condensed Matter 1981*, American Institute of Physics, 1982, pp. 251-266.

4. Bauer, F., "Method and Device for Poling Ferroelectric Materials," U.S. Patent 4,611,260, 9 Sep 1986.

5. Bauer, F., "Device for Poling Ferroelectric Materials," U.S. Patent 4,684,337, 4 Aug 1987.

6. Graham, R. A.; Anderson, M .U.; Bauer, F.; and Setchell, R.E., "Piezoelectric Polarization of the Piezoelectric Polymer PVDF from 10 MPa to 10 GPa: Studies of Loading Path Dependence," *Shock Compression of Condensed Matter 1991*, Elsevier Science Publishers, B.V., 1992, pp. 883-886.

7. Bauer, F.; Graham, R. A.; Anderson, M. U.; Lefebvre, H.; Lee, L. M.; and Reed, R.P., "Response of the Piezoelectric Polymer PVDF to Shock Compression Greater than 10 GPa," *Shock Compression of Condensed Matter 1991*, Elsevier Science Publishers, B.V., 1992, pp. 887-890.

8. Bauer, F., and Lichtenberger, A., "Use of PVF_2 Shock Gauges for Stress Measurements in Hopkinson Bar," *Shock Waves in Condensed Matter 1987*, Elsevier Science Publishers, B.V., 1988, pp. 631-634.

9. Gustavson, P. K.; Tasker, D. G.; and Forbes, J. W., "Underwater Shock Wave Measurements Using PVDF ansducers," *Shock Compression of Condensed Matter 1991*, Elsevier Science Publishers, B.V., 1992, pp. 905-908.

10. Sandusky, H.W., personal communication.

11. Bernecker, R. R.; Sandusky, H. W.; Clairmont Jr., A. R.; and Groves, C. L., *Calibration of Shock Loading from a Variety of Pressed Pentolite Donors in a Water Environment*, NAVSWC TR 89-358, in press.

12. Erkman, J. O.; Christensen, A. B.; and Fowles, G. R., *Attenuation of Shock Waves in Solids*, AFWL-TR-66-12, 1966.

REFERENCES (CONT.)

13. Lemar, E. R., personal communication.

14. Setchell, R. E., "Response of Polyvinylidene Fluoride (PVF_2) Gauges to Structured Waveforms," *Shock Waves in Condensed Matter 1987*, Elsevier Science Publishers, B.V., 1988, pp. 623-626.

APPENDIX A

LOW INDUCTANCE PVDF SENSOR DESIGN

SENSOR DESIGN

The low inductance Naval Surface Warfare Center (NAVSWC) sensor design had wide, short, triangular connections that fanned out from the central sensor area (see Figure A-1). A 1.5 mm space separated adjacent triangles. This design was called the "double maltese-cross." The central active area was 5 mm in diameter, and the PVDF film was 26 μm thick. The sensor was designed to have an inductance of 3 nH from the active area to the outside periphery. The inductance was calculated by adapting the methods of Rosa and Gray.[A-1,A-2] Indeed, the measured inductance was 3 nH.

The connections to the central circle were made by relatively narrow lines from the triangular electrodes. The electrodes were vacuum-deposited onto the PVDF, first an approximately 25 nm of chromium, then an approximately 100 nm layer of gold.[A-3,A-4] In Figure A-1 the gold surfaces are shown in white whereas the gray shaded regions are chromium viewed through the PVDF.

SENSOR PREPARATION

Ten sensors were prepared by Bur and Roth[A-3,A-4] with mean remanent polarization of 6.00 $\mu C/cm^2$ to a precision of 0.5 percent. The PVDF film was manufactured by Rhone-Poulenc and was obtained from a selected master batch which is kept at Sandia National Laboratories by R. Graham. X-ray observations and measurements of density[A-3] indicated that the material was biaxially oriented, containing both nonpolar α and polar β crystalline phases and had a crystallinity of 50 percent. The as-received material had a density at room temperature of 1.306 g/cm^3. The sensors were poled by the Bauer polarization procedure.[A-5]

Bur and Roth also discovered from density and x-ray measurements that the crystallinity remained constant during poling but with a significant conversion of α phase crystallites to the polar β phase. They observed that each sensor required a unique maximum poling field to achieve the same remanent polarization. This contributed to the presence of different distributions and amounts of space charge in each sensor. The observed increase in the saturation polarization, with increase in the maximum poling field, is also attributed to the effect of space charge. This charge resides at the surface of polar crystals and creates a local electric field which diminishes the effect of the applied poling field. Their attempts to increase the remanent polarization to values of 8.0 $\mu C/cm^2$ and greater were not successful because dielectric breakdown occurred at the edges of the electrodes before reaching this level of polarization.

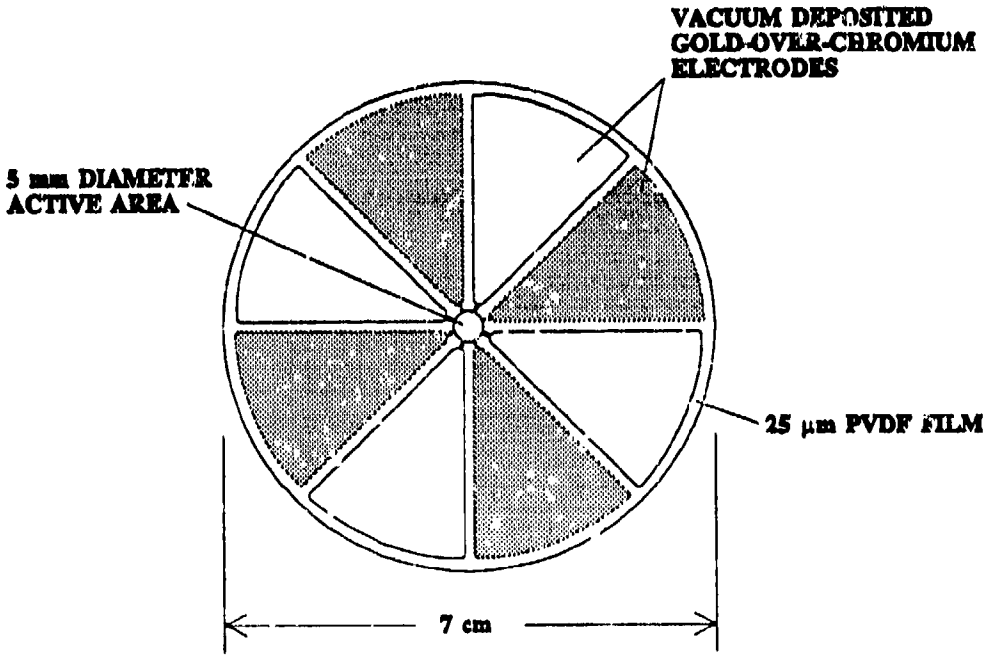

FIGURE A-1. NAVSWC DOUBLE MALTESE CROSS SENSOR

LATER DESIGN

The new NAVSWC sensor was designed to reduce the dielectric breakdown problems of the first design. The central area was a 5 mm diameter octagon. The connections were 5 mm in width and comprised two crosses, one on each side of the PVDF, intersecting at 45°. The area of intersection of the two crosses was the octagon. The remaining electrodes were the same triangular sectors of the earlier design. This new design was never built.

UNDERWATER EXPERIMENT

The double maltese-cross design was tested in a series of underwater experiments.[A-6] The sensors were placed close to the surface of a 41 mm diameter Pentolite sphere. This sphere was a standard donor used for the NAVSWC underwater sensitivity test. The pressure/distance relationship for the test had already been determined using streak photography and lithium niobate sensors.[A-7,A-8] The sensors were suspended from a connecting ring which incorporated a double-sided printed circuit board. The board allowed low inductance connections to be made between the PVDF sensor, the terminating capacitor and resistor, and the cable.

The PVDF surfaces were insulated from the water with Saran wrap attached by a smear of silicone grease to exclude air. The circuit board was protected with silicone rubber (RTV 3145) and insulating tape.

A voltage record from one experiment is shown in Figure A-2. This record was obtained using an integrating capacitor of 100 nF mounted directly on the sensor and matched to a 50 Ω, RG58 cable with a matching series resistor as shown previously in Figure 3-1 of the main text.

In these preliminary experiments, no allowance was made for sensor strain effects.

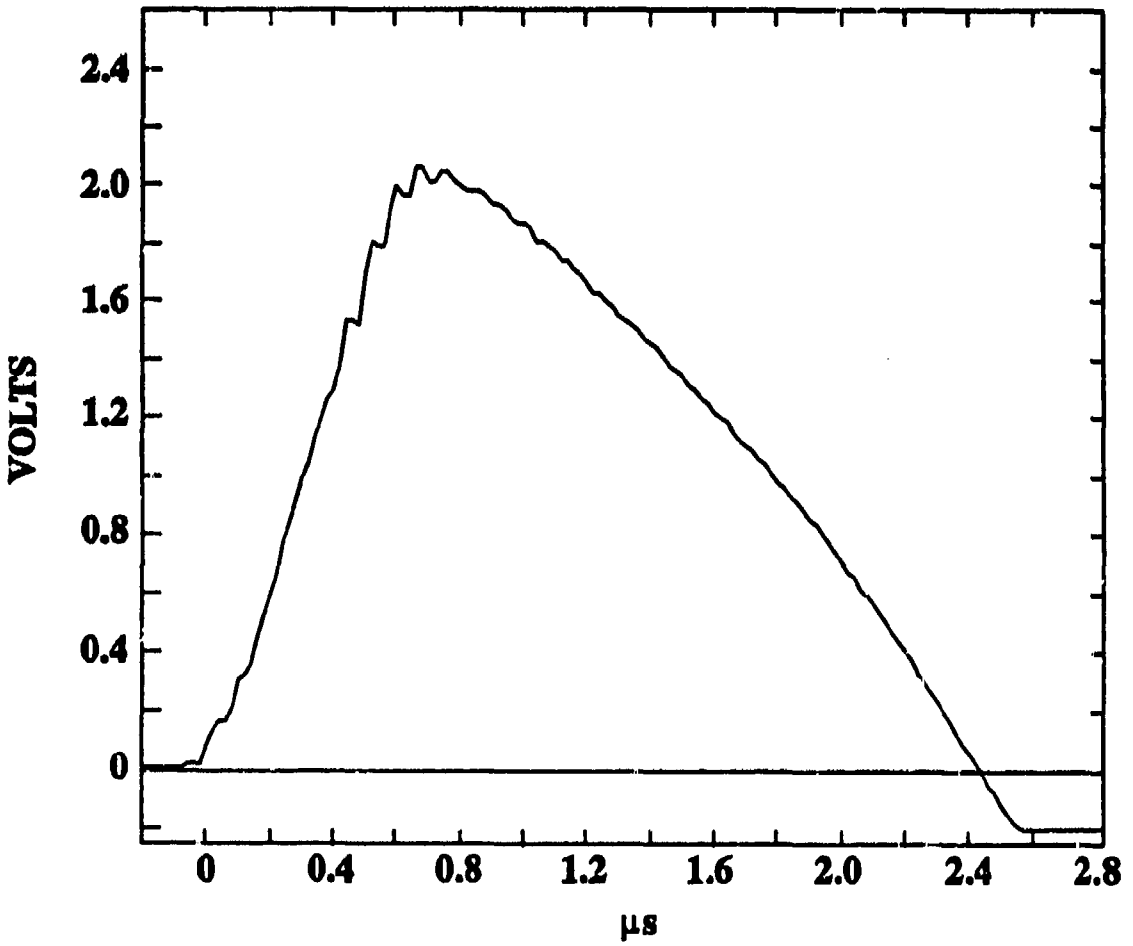

FIGURE A-2. UNDERWATER SHOCK WAVE MEASURED WITH THE NAVSWC DOUBLE MALTESE-CROSS SENSOR

REFERENCES

A-1. Rosa, E. B.,"On the Geometrical Mean Distances of Rectangular Area and the Calculation of Self-Inductance," Bureau of Standards Bulletin, Vol. 3, 1907, pp. 5-41.

A-2. Gray, A., "Calculation of Coefficients of Induction, Absolute Measurements II," Part II, pp. 288-306 (note the misprints cited by Rosa).

A-3. Bur, A. J., and Roth, S. C., "Preparation of Thin Film Polyvinylidene Fluoride Shock Wave Pressure Transducers," NBSIR 87-3680, National Bureau of Standards, Dec 1987.

A-4. Bur, A. J., and Roth, S. C., "Preparation of Thin Film Polyvinylidene Fluoride Shock Wave Pressure Transducers," Bull. APS, Vol. 33, No. 3, 1988, p. 582.

A-5. Bauer, F., "PVF_2 Polymers: Ferroelectric Polarization and Piezoelectric Properties under Dynamic Pressure and Shock Wave Action," *Ferroelectrics*, Vol. 49, 1983, p. 231.

A-6. Forbes, J. W.; Tasker, D. G.; and Gustavson, P., "A New Fast PVDF Pressure Gauge," Bull. APS, Vol. 33, No. 3, 1988, p. 582.

A-7. Liddiard, T. P., and Forbes, J. W., *Shock Waves in Fresh Water Generated by the Detonation of Pentolite Spheres*, NSWC TR 82-488, 26 May 1983.

A-8. Liddiard, T. P., and Forbes, J. W., "Shockwaves in Fresh Water Generated by the Detonation of Pentolite Spheres," *Shock Waves in Condensed Matter-1981*, AIP No. 78, 1982.

DISTRIBUTION

	Copies
DOD ACTIVITIES (CONUS)	
ATTN F MENZ USD (A) DDRE (R AT ET) STAFF SPECIALIST FOR WEAPONS TECHNOLOGY THE PENTAGON WASHINGTON DC 20301	1
ATTN R SIEWART OUSDRE R&AT MST THE PENTAGON WASHINGTON DC 20301	1
ATTN G KOPCSAK (OM) D ANDERSON (NW&M) OUSDRE TWP THE PENTAGON WASHINGTON DC 20301	1 1
ATTN SURFACE WARFARE AIR WARFARE SUBS ASW OASN RE&S THE PENTAGON WASHINGTON DC 20301	1 1 1
ATTN I BLATSTEIN (TD) NAVAL SURFACE WARFARE CENTER WASHINGTON DC 20362	1
DEFENSE TECHNICAL INFORMATION CENTER CAMERON STATION ALEXANDRIA VA 22304-6145	12
ATTN GIFT AND EXCHANGE DIV LIBRARY OF CONGRESS WASHINGTON DC 20540	4
ATTN TECHNICAL LIBRARY DIRECTOR DEFENSE RESEARCH AND ENGINEERING WASHINGTON DC 20305	1
ATTN TECHNICAL LIBRARY INSTITUTE FOR DEFENSE ANALYSES 1801 N BEAUREGARD ST ALEXANDRIA VA 22311	1
ATTN LIBRARY DIRECTOR DEFENSE ADVANCED RESEARCH PROJECTS OFFICE 1400 WILSON BOULEVARD ARLINGTON VA 22209	1
ATTN TECHNICAL LIBRARY SPSP P CASTLEBERRY SPSP J CONNELL SPSD J DEPLITCH SPSD K GOERING SPSD K STEIN SPSP M FRANKEL SPSP T FREDRICKSON SP C MCFARLAND DIRECTOR DEFENSE NUCLEAR AGENCY WASHINGTON DC 20305	1 1 1 1 1 1 1 1 1
ATTN J D RENICK DEFENSE NUCLEAR AGENCY FIELD COMMAND KIRTLAND AFB NM 87115	1

DISTRIBUTION (Continued)

	Copies
ATTN DDESB KT	1
DDESB KT1 J WARD	1
DEPARTMENT OF DEFENSE	
EXPLOSIVE SAFETY BOARD	
HOFFMAN BUILDING 1	
2461 EISENHOWER AVENUE	
ALEXANDRIA VA 22331-0600	
ATTN TECHNICAL LIBRARY	1
A WILLIAMS	1
COMMANDING OFFICER	
NAVAL RESEARCH LABORATORY	
WASHINGTON DC 20350-5000	
ATTN R WHITLOCK	1
CONDENSED MATTER PHYSICS	
BRANCH	
NAVAL RESEARCH LABORATORY	
WASHINGTON DC 20375-5000	
ATTN M KAHN	1
MATERIALS DIVISION	
NAVAL RESEARCH LABORATORY	
WASHINGTON DC 20375-5000	
ATTN ONR 3322 R MILLER	1
ONR 4410 P QUINN	1
ONR 4400 E ZIMET	1
ONR 4423 D SIEGEL	1
ONR 4200 A FAULSTICH	1
ONR 4425 D HOUSER	1
OFFICE OF THE CHIEF OF NAVAL	
RESEARCH	
800 N QUINCY ST BCT1	
ARLINGTON VA 22217-5000	
ATTN OP 005	1
OP 021	1
OP 03	1
OP 035	1
OP 0354	1
OP 07	1
OP 987B	1
CHIEF OF NAVAL OPERATIONS	
WASHINGTON DC 20350	

	Copies
ATTN SPAWAR 05	1
COMMANDER	
SPACE AND NAVAL WARFARE	
SYSTEMS COMMAND	
WASHINGTON DC 20363-5100	
ATTN SEA 05R	1
SEA 06APR MUIR	1
SEA 06B	1
SEA 06R	1
SEA 06U	1
SEA 62	1
SEA 62Z31E SCHONER	1
SEA 662	1
SEA 6622	1
SEA 665	1
SEA 6652	1
SEA 99612	1
PMS 422 16 LUBIN	1
PMS 422G	1
CHENG T1 RITTER	1
COMMANDER	
NAVAL SEA SYSTEMS COMMAND	
WASHINGTON DC 20362-5105	
ATTN AIR 540	1
AIR 540TF	1
AIR 5404	1
AIR 54051	1
AIR 54043	1
TECHNICAL LIBRARY	1
COMMANDER	
NAVAL AIR SYSTEMS COMMAND	
WASHINGTON DC 20361	
COMMANDING OFFICER	
NAVAL INTELLIGENCE SUPPORT	
CENTER	
4302 SUITLAND ROAD	
WASHINGTON DC 20390-5140	1
COMMANDING OFFICER	
SEAL TEAM 2	
FPO AE 09510-4633	1

DISTRIBUTION (Continued)

	Copies
ATTN TECHNICAL LIBRARY	1
R GARRISON	1
S WANG	1
JW SYKES	1
W CONLEY	1
F FISCH	1
CODE 17	1
CODE 172	1
COMMANDER	
NAVAL SURFACE WARFARE CENTER	
CARDEROCK DIVISION	
BETHESDA MD 20084	
ATTN CODE 2730D	1
TECHNICAL LIBRARY	1
J CHANG	1
P DENDOR	1
S MITCHELL	1
L NEWMAN	1
COMMANDING OFFICER	
NAVAL SURFACE WARFARE CENTER	
INDIAN HEAD DIVISION	
INDIAN HEAD MD 20640	
ATTN TECHNICAL LIBRARY	1
COMMANDING OFFICER	
NAVAL EXPLOSIVES ORDNANCE	
DISPOSAL TECHNOLOGY CENTER	
INDIAN HEAD MD 20640	
ATTN TECHNICAL LIBRARY	1
CODE 363 R NADOLINK	1
COMMANDER	
NAVAL UNDERWATER WARFARE	
CENTER DIVISION	
NEWPORT RI 02841-5047	
ATTN TECHNICAL LIBRARY	1
PRESIDENT	
NAVAL WAR COLLEGE	
NEWPORT RI 02841	

	Copies
ATTN CODE 177	1
TECHNICAL LIBRARY	1
COMMANDER	
DAVID TAYLOR RESEARCH CENTER	
UERD	
PORTSMOUTH VA 23709	
ATTN LIBRARY	1
CODE 470A	1
CODE 35	1
M KRAM	1
L LEONARD	1
J ZEHMER	1
J ROUDABUSH	1
OFFICER IN CHARGE	
INDIAN HEAD DIVISION	
NAVAL SURFACE WARFARE CENTER	
YORKTOWN DETACHMENT	
YORKTOWN VA 23691-5110	
ATTN TECHNICAL LIBRARY	1
COMMANDING OFFICER	
NAVAL SURFACE WARFARE CENTER	
NAVAL COASTAL SYSTEMS STATION	
PANAMA CITY FL 32407-5000	
ATTN LIBRARY	1
COMMANDING GENERAL	
MARINE CORPS DEVELOPMENT AND	
EDUCATION COMMAND	
MARINE CORPS LANDING FORCE	
DEVELOPMENT CENTER	
QUANTICO VA 22134	
ATTN LIBRARY	1
CODE 3031 E NEAL	1
CODE 50D A NORRIS	1
CODE 505 J SHORT	1
CODE 90 A WHITNER	1
COMMANDING OFFICER	
NAVAL SURFACE WARFARE CENTER	
CRANE DIVISION	
CRANE IN 47522	

DISTRIBUTION (Continued)

	Copies
ATTN CODE 32	1
CODE 3205 F MARKARIAN	1
CODE 3205 S DEMAY	1
CODE 3208	1
CODE 321	1
CODE 32103	1
CODE 3211	1
CODE 3212	1
CODE 3212 E LUNDSTROM	1
CODE 3213	1
CODE 3213 T ATIENZA MOORE	1
CODE 3213 H JOHN	1
CODE 3214	1
CODE 326 MCCUBBIN	1
CODE 326B L JOSEPHSON	1
CODE 3261 WEEKS	1
CODE 3261 FASIS	1
CODE 3261 BUCKLEY	1
CODE 3263	1
CODE 3264	1
CODE 327	1
CODE 32904 STEPHENS	1
CODE 3293 COPE	1
CODE 3293 MAURER	1
CODE 381	1
CODE 385	1
CODE 3850	1
CODE 3853	1
CODE 389 T BOGGS	1
CODE 38906 PEARSON	1
CODE 3891 M CHAN	1
CODE 3984 ALEXANDER	1
CODE 3894 M WAGENHALS	1
CODE 3894 A LINDFORS	1
CODE 39	1
CODE 3917	1
TECHNICAL LIBRARY	1
COMMANDER	
NAVAL AIR WARFARE CENTER	
WEAPONS DIVISION	
CHINA LAKE CA 93555-6001	
ATTN CODE 2145	1
COMMANDER	
PACIFIC MISSILE TEST CENTER	
POINT MUGU CA 93042	
ATTN TECHNICAL LIBRARY	1
COMMANDER	
NAVAL COMMAND AND CONTROL	
OCEAN SURVELLIANCE CENTER	
SAN DIEGO CA 92152-5000	
COMMANDING OFFICER	
NAVAL SURFACE WARFARE CENTER	
PORT HUENEME DIVISION	
PORT HUENEME CA 93043	1
ATTN LIBRARY	1
SUPERINTENDENT	
NAVAL POSTGRADUATE SCHOOL	
MONTEREY CA 93940	
COMMANDING OFFICER	
NAVAL UNDERSEA WARFARE	
DIVISION	
KEWPORT WA 98345-0580	1
COMMANDER	
NAVAL WEAPONS EVALUATION	
FACILITY	
KIRTLAND AIR FORCE BASE	
ALBUQUERQUE NM 87117	1
ATTN LIBRARY	1
DELHD DE OM K WARNER	1
COMMANDING OFFICER	
HARRY DIAMOND LABORATORIES	
2800 POWDER MILL ROAD	
ADELPHI MD 20783	
ATTN AMSMI RD ST WF D LOVELACE	1
COMMANDER	
US ARMY MISSILE COMMAND	
REDSTONE ARSENAL AL 35898-5247	
ATTN DRXSY D	1
DRXSY J J MCCARTHY	1
DIRECTOR	
ARMY MATERIALS SYSTEMS	
ANALYSIS AGENCY	
ABERDEEN PROVING GROUND	
MD 21005	

DISTRIBUTION (Continued)

	Copies
ATTN SMCCR DDP	1
COMMANDER	
US ARMY CHEMICAL RESEARCH	
DEVELOPMENT AND	
ENGINEERING CENTER	
ABERDEEN PROVING GROUND	
MD 21010-5423	
ATTN DRDAR BLP	1
SLCRB TB E	1
SLCRB IB I P KASTE	1
V BOYLE	2
R FREY	1
J FRASIER	1
F GRACE	1
W HILLSTROM	1
R JAMIESON	1
J STARKENBERG	1
H REEVES	1
L VANDEKIEFT	1
W WALTERS	1
J WATSON	1
TECHNICAL LIBRARY	1
STINFO OFFICE	1
COMMANDING OFFICER	
ARMY BALLISTIC RESEARCH LAB	
ABERDEEN PROVING GROUND	
MD 21005	
ATTN DRSMC TD	1
DDRSMC LCE2	1
DRDSMC LCE E BAKER	1
DRSMC LCE C	1
DRSMC LCE D2	1
DRSMC LCM2	1
DRSMC LCM SAR	1
WESTERDAHL	1
DRSMC LCU2	1
DRSMC LCU E	1
COMMANDER	
US ARMY ARMAMENT RESEARCH	
DEVELOPMENT AND	
ENGINEERING CENTER	
DOVER NJ 07806-5000	

	Copies
ATTN AMSLC TD R VITALI	1
COMMANDER	
US ARMY LABORATORY COMMAND	
2800 POWDER MILL ROAD	
ADELPHI MD 20783-1145	
ATTN G R HUSK	1
COMMANDER	
US ARMY RESEARCH OFFICE	
PO BOX 12211	
RESEARCH TRIANGLE PARK	
NC 27709-2211	
ATTN T MATUSKO	1
COMMANDER	
AIR FORCE OFFICE OF SCIENTIFIC	
RESEARCH	
BOLLING AIR FORCE BASE	
WASHINGTON DC 20332	
ATTN AFIS INTAW MAJ R ESAW	1
COMMANDER	
AIR FORCE INTELLIGENCE SERVICE	
BOLLING AIR FORCE BASE	
WASHINGTON DC 20332-5000	
ATTN C MERRILL	1
F ROBERTO	1
COMMANDER	
AIR FORCE ASTRONAUTICS	
LABORATORY	
ATAL MKPL	
EDWARDS AFB CA 93521	
ATTN WL MNF R BOULET	1
R ERHART	1
WL MNW E POSTON	1
WL MNE S AUBERT	1
J CORLEY	1
G GLENN	1
R MCKENNEY JR	1
I G PARSONS	1
MSD SES F WEST	1
MSD XRS J JENNS JR	1
COMMANDER	
AFATL MN	
EGLIN AFB FL 32542-5434	

DISTRIBUTION (Continued)

	Copies
NON-DOD ACTIVITIES	
CENTER FOR NAVAL ANALYSIS 4401 FORD AVENUE ALEXANDRIA VA 22302-0268	1
ATTN R WATSON DEPARTMENT OF THE INTERIOR BUREAU OF MINES PITTSBURGH RESEARCH CENTER COCHRANS MILL ROAD PITTSBURGH PA 15236-0070	1
ATTN L53 H JEAN HIGHBY	1
K BAHL	1
P CRAWFORD	1
L GREEN	1
J HUMPHREY	1
J KURY	1
E LEE	1
K SCRIBNER	1
R SIMPSON	1
W TAO	1
C TARVER	1
P URTIEW	1
R WEINGART UNIVERSITY OF CALIFORNIA LAWRENCE LIVERMORE NATIONAL LABORATORY PO BOX 808 LIVERMORE CA 94550	1
ATTN DARLENE M LOLL FOR TECHNICAL LIBRARY SANDIA NATIONAL LABORATORY PO BOX 969 LIVERMORE CA 94550-0096	1
ATTN E AUSTIN TECH LIBRARY REPORTS RECEIVING CLERK SANDIA NATIONAL LABORATORY PO BOX 5800 ALBUQUERQUE NM 87185	1
ATTN LIBRARIAN	1
E LISZKA APPLIED RESEARCH LABORATORY PENNSYLVANIA STATE UNIVERSITY PO BOX 30 UNIVERSITY PARK STATE COLLEGE PA 16804	1
ATTN T W CHRISTIAN THE JOHNS HOPKINS UNIVERSITY APPLIED PHYSICS LABORATORY CHEMICAL PROPULSION INFORMATION AGENCY JOHNS HOPKINS ROAD LAUREL MD 20707-6099	1
ATTN TECHNICAL LIBRARY	1
DEANNA JONES JOHNS HOPKINS UNIVERSITY APPLIED PHYSICS LABORATORY JOHNS HOPKINS ROAD LAUREL MD 20707-6099	1
ATTN SECURITY ADMINISTRATOR	1
ELIZABETH A TILL	1
CODE TERA M KEMPTON	1
CODE CETR T JOYNER	1
P PERSSON NEW MEXICO INSTITUTE OF MINING TECHNOLOGY CAMPUS STATION SOCORRO NM 87801	2
ATTN P E WILLIAMS NEW MEXICO INSTITUTE OF MINING AND TECHNOLOGY ENERGETIC MATERIALS RESEARCH AND TESTING CENTER SOCORRO NM 87801	1

DISTRIBUTION (Continued)

	Copies
ATTN M 8	1
MST DO MS G 756	1
R ALCON	1
I ASAY	1
J BDZIL	1
A BOWMAN	1
G BUNTAIN	1
L CHAPMAN	1
M COBURN	1
J DAVIS	1
J DICK	1
B DOBRATZ	1
C FOREST	1
J GOFORTH	1
J HOPSON	1
P HOWE	1
J N JOHNSON	1
J KENNEDY	1
T LARSON	1
W MAUTZ	1
S PETERSON	1
R RABIE	1
J REPA	1
S SHEFFIELD	1
L STRETZ	1
P TANG	1
M URIZAR	1
J WACKERLE	1
LOS ALAMOS NATIONAL LABORATORY PO BOX 1663 LOS ALAMOS NM 87545	
ATTN G CHIN	1
AEROJET ORDNANCE AND MANUFACTURING COMPANY 9236 EAST HALL ROAD DOWNEY CA 90241	
ATTN KENNETH GRAHAM	1
ATLANTIC RESEARCH CORPORATION 5945 WELLINGTON ROAD GAINESVILLE VA 22065-1699	
ATTN F LASCHER	1
E MOULIC	1
AVCO TECHTRON SYSTEMS INC 201 LOWELL STREET WILMINGTON MA 01887	
ATTN JOSEPHINE HUGGINGS	1
BATELLE MEMORIAL LABORATORY TACTICAL TECHNOLOGY CENTER 505 KING AVENUE COLUMBUS OH 43201	
ATTN E WILHELM	1
R HELZER	1
BOEING AEROSPACE COMPANY PO BOX 3707 SEATTLE WA 98124	
ATTN R SEWELL	1
COMARCO INC WEAPON SUPPORT DIVISION RIDGECREST CA 93555	
ATTN J MOSCHEL	1
C STROSBERG	1
J MEIER	1
M BRAMMER	1
CHAMBERLAIN MFG CORP 550 ESTHER STREET WATERLOO IA 50704-2524	
ATTN R WEST	1
P CHOU	1
DYNA EAST CORPORATION 320 ARCH STREET PHILADELPHIA PA 19104-2588	
ATTN SAM MIGUEL	1
FORD AEROSPACE AND COMMUNICATIONS CORPORATION AERONAUTRONIC DIVISION FORD ROAD JAMBOREE NEWPORT BEACH CA 92658-9983	

DISTRIBUTION (Continued)

	Copies
ATTN G WILLIAMS HERCULES INCORPORATED ROCKET CENTER PO BOX 210 ROCKET CENTER WV 26726	1
ATTN M KLAKKEN	1
M BERGER	1
G BUTCHER	1
L LOSEE	1
T SPEED HERCULES BACCHUS WORKS MAGNA UT 84044-0098	1
ATTN L WEBER HUGHES AIRCRAFT INC MISSILE SYSTEMS GROUP 8433 FALLBROOK AVENUE CANOGA PARK CA 91304-9976	1
ATTN TIMOTHY PENDERGRASS KAMAN SCIENCES CORP 600 BLVD SOUTH SUITE 208 HUNTSVILLE AL 35802	1
ATTN J CZECHANSKI INTERFEROMETRICS INC 8150 LEESBURG PIKE VIENNA VA 22182-2799	1
ATTN D JONES THIOKOL CORPORATION MATERIALS AND PROCESS DEVELOPMENT HUNTSVILLE DIVISION PO BOX 400006 HUNTSVILLE AL 35815-1506	1
D R KENNEDY ASSOCIATES PO BOX 4003 MOUNTAIN VIEW CA 94040	1
RADKOWKSI ASSOCIATES P O BOX 5474 RIVERSIDE CA 92517	1
KORNHAUSER CONSULTING SERVICES 620 ARGYLE AVENUE WYNNEWOOD PA 19096	1
ATTN R HODGES	1
J SMITH LOCKHEED MISSILES & SPACE CO PO BOX 504 SUNNYVALE CA 94086	1
ATTN J FLOWERS LTV AEROSPACE & DEFENSE CO LTV AEROSPACE PRODUCTS GROUP PO BOX 655907 DALLAS TX 95265-5907	1
ATTN H FUEHRER MARTIN MARIETTA CORPORATION ORLANDO AEROSPACE MISSILE SYSTEMS PO BOX 555837 ORLANDO FL 32855	1
ATTN T KITCHEN ORLANDO TECHNOLOGY INC PO BOX 855 SHALIMAR FL 32579	1
ATTN W ZARR RAYTHEON COMPANY HARTWELL ROAD BEDFORD MA 01730	1
ATTN R SEDGWICK S CUBED A DIVISION OF MAXWELL LABS INC PO BOX 1620 LAJOLLA CA 92038	1
ATTN D GARFINKLE SCIENCE APPLICATIONS INTERNATIONAL 26679 W AGOURA ROAD CALABASAS CA 91302	1

DISTRIBUTION (Continued)

	Copies
ATTN K L CHRISTIANSON	1
J L HOULTON	1
G JOHNSON	1
ALLIANT TECHSYSTEMS INC	
7225 NORTHLAND DRIVE	
BROOKLYN PARK MN 55428	
ATTN C ANDERSON	1
H GRYTING	1
A WENTZEL	1
SOUTHWEST RESEARCH INSTITUTE	
PO DRAWER 28510	
SAN ANTONIO TX 78284	
ATTN D CURRAN	1
D SHERWOOD	1
M COWPERTHAWAITE	1
SRI INTERATIONAL	
333 RAVENSWOOD AVENUE	
MENLO PARK CA 94025	
ATTN L WEBER	1
J NEWQUIST	1
TELEDYNE BROWN ENGINEERING	
PO BOX 070007	
HUNTSVILLE AL 35807	
ATTN R CHURCH	1
TRW	
SAN BERNADINO CA 92401	
ATTN G WEEDING	1
UNIVERSITY OF DENVER	
COLORADO SEMINARY	
PO BOX 10758	
DENVER CO 80210	
ATTN A MELLOR	1
VANDERBILT UNIVERSITY	
NASHVILLE TN 37235	
ATTN L ZERNOW	1
ZERNOW TECHNICAL SERVICES INC	
PO BOX 54	
SAN DIMAS CA 91773	

	Copies
ATTN H ADOLPH	1
S JACOBS	1
J W WATT	1
ADVANCED TECHNOLOGY AND RESEARCH INC	
LAUREL TECHNOLOGY CENTER	
14900 SWEITZER LANE	
LAUREL MD 20707	
ATTN W SMITH	1
ADVANCED TECHNOLOGY INC	
2121 CRYSTAL DRIVE	
ARLINGTON VA 22202	
ATTN R DICK	1
UNIVERSITY OF MARYLAND	
DEPARTMENT OF MECHANICAL ENG	
COLLEGE PARK MD 20742	
ATTN P J DIBONA	1
FMC CORPORATION	
NAVAL SYSTEMS DIVISION M170	
4800 EAST RIVER ROAD	
MINNEAPOLIS MN 55421	
ATTN D DAVISON	1
SHOCK TRANSIENTS INC	
PO BOX 5357	
HOPKINS MN 55343	
ATTN J ENIG	1
ENIG ASSOCIATES INC	
SUITE 500	
11120 NEW HAMPSHIRE AVENUE	
SILVER SPRING MD 20904-2633	
ATTN S EIDELMAN	1
SCIENCE APPLICATIONS INTERNATIONAL CORP	
1710 GOODRIDGE DRIVE	
MCLEAN VA 22102	
ATTN M GUNGER	1
ORLANDO TECHNOLOGY INC	
PO BOX 855	
SHALIMAR FL 32579	

DISTRIBUTION (Continued)

	Copies
ATTN P JONES	1
THE BRITISH EMBASSY	
BRITISH DEFENCE STAFF	
3100 MASSACHUSETTS AVENUE NW	
WASHINGTON DC 20008	
ATTN M ANDERSON	1
L CHHABILDAS	1
D GRADY	1
R GRAHAM	1
J GREENWOLL	1
R REED	1
R SETCHELL	1
SANDIA NATIONAL LABORATORIES	
ALBUQUERQUE NM 87185-5800	
ATTN Y GUPTA	1
SHOCK DYNAMICS LABORATORY	
WASHINGTON STATE UNIVERSITY	
PULLMAN WA 99164-2814	
ATTN D SOLIE	1
J JOHNSON	1
P DUTTA	1
J KALAFUT	1
US ARMY CORPS OF ENGINEERS	
COLD REGIONS RESEARCH AND ENGINEERING LABORATORY	
HANOVER NH 03755-1290	
ATTN J CHAREST	1
C LYNCH	1
DYNASEN INC	
20 ARNOLD PL	
GOLETA CA 93117	
ATTN A BUR	1
T DAVIS	1
A DEREGG	1
B DICKENS	1
S ROTH	1
NATIONAL INSTITUTE OF STANDARDS AND TECHNOLOGY	
POLYMERS DIVSION	
GAITHERSBURG MD 20899	

	Copies
NON-DOD ACTIVITIES (EX-CONUS)	
ATTN LIBRARY	1
ET1 BLDG X3 M D COOK	1
ET BLDG X59 A CUMMINGS	1
B HAMMANT	1
ET1 BLDG X51 P HASKINS	1
G HOOPER	1
ET1 BLDG X60 D MULLENGER	1
DEFENSE RESEARCH AGENCY	
FORT HALSTEAD SEVENOAKS	
KENT TN14 7BP	
UNITED KINGDOM	
ATTN LIBRARY	1
H R JAMES	1
ATOMIC WEAPONS ESTABLISHMENT	
FOULNESS ISLAND	
ESSEX SS3 9XE	
UNITED KINGDOM	
ATTN J JENKINS	1
B D LAMBOURN	1
D C SWIFT	1
MOD(PE)	
ATOMIC WEAPONS ESTABLISHMENT	
AWE(A)	
ALDERMASTON	
READING BERKSHIRE RG7 4PR	
UNITED KINGDOM	
ATTN R STENSON (S DIV)	1
ORDNANCE BOARD	
EMPRESS STATE BUILDING	
LILLIE ROAD LONDON SW6 1TR	
UNITED KINGDOM	
ATTN J COOPER	1
G A LEIPER	1
I J KIRBY	1
ICI EXPLOSIVES	
STEVENSTON KA20 3LN	
UNITED KINGDOM	

DISTRIBUTION (Continued)

	Copies
ATTN W LEEMING	1
NEC	
ARDEER SITE	
STEVENSTON AYRESHIRE KA20 3LN	
SCOTLAND	
ATTN M CHICK	1
D D RICHARDSON	1
D A JONES	1
M PODLESAK	1
MATERIAL RESEARCH LABORATORY	
PO BOX 50	
ASCOT VALE VICTORIA 3032	
AUSTRALIA	
ATTN D L KENNEDY	1
ICI EXPLOSIVES	
BALLARAT ROAD	
DEER PARK VICTORIA 3023	
AUSTRALIA	
ATTN J N OECONOMOS	1
F CHAISSE	1
CEA	
CENTRE D'ETUDES	
DE VAUJOURS-MORONVILLIERS	
B P N° 7 77181 COURTRY	
FRANCE	
ATTN F BAUER	1
INSTITUT FRANCO-ALLEMAND DE	
SAINT-LOUIS (ISL)	
12 RUE DE L'INDUSTRIE	
68300 SAINT-LOUIS	
FRANCE	
ATTN P CHARTAGNAC	1
P DECASO	1
B JIMENEZ	1
DGA/CENTRE D'ETUDES DE GRAMAT	
46500 GRAMAT	
FRANCE	

	Copies
ATTN M BOUCHU	1
C CAVAILLER	1
J DELAVAL	1
CEA/CENTRE D'ETUDES DE	
VAUJOURS-MORONVILLIERS	
FRANCE	
ATTN M HELD	1
MESSERSCHMITT-BOLKOW-BLOHM	
GMBH	
RESEARCH DEPARTMENT	
8898 SCHROBENHAUSEN	
GERMANY	
ATTN CONRAD BELANGER	1
ROCCO FARINACCIO	1
IRENE HOOTON	1
GRANT MCINTOSH	1
DEFENSE RESEARCH	
ESTABLISHMENT VALCARTIER	
PO BOX 8800	
COURCELETTE QUEBEC	
CANADA	
G0A 1R0	

INTERNAL

C72W		1
E231		2
E232		3
G10		1
G13	D L DICKINSON	1
G13	T WASMOND	1
G20		1
G22		1
G22	C GARNETT	1
G22	W HOLT	1
G22	W MOCK	1
G22	T SMITH	1
G22	T SWIERK	1
G22	S WAGGENER	1
G22	L WILSON	1
G822	O PARRENT	1

DISTRIBUTION (Continued)

		Copies
G83	L LIPTON	1
G91		1
G91	W FURR	1
G91	R PLENGE	1
G91	D HINELY	1
G91	J JEROSKI	1
G92	D BETANCOURT	1
G92	J BURNS	1
G92	H CHEN	1
G92	A DARE	1
G92	R GODZUK	1
G92	W HINCKLEY	1
G92	A KOENIGSBERG	1
G92	K MCDONALD	1
G92	R MCKEOWN	1
G92	J MENTGES	1
G92	T MOORE	1
G92	C NIGGINS	1
G92	B PARK	1
G92	C SMITH	1
G92	D TAM	1
G92	L TAYLOR	1
G92	W WALKER	1
R		1
R01		1
R04		1
R06		1
R10		1
R101		1
R102		1
R10A2	S COLLIGNON	1
R10B		1
R11		1
R11	E ANDERSON	1
R11	D CICHRA	1
R11	F GALLANT	1
R11	J GOLDWASSER	1
R11	C GOTZMER	1
R11	N JOHNSON	1
R11	J LEAHY	1
R11	L NOCK	1
R11	Y TRAN	1
R12		1
R12	B GLANCY	1
R12	J LAIB	1
R13		1
R13	R BAKER	1
R13	R BERNECKER	1
R13	R BARDO	1
R13	C COFFEY	1
R13	J DAVIS	1
R13	D DEMSKE	1
R13	J FORBES	10
R13	R GUIRGUIS	1
R13	H JONES	1
R13	RICHARD LEE	1
R13	E LEMAR	3
R13	T LIDDIARD	1
R13	P MILLER	1
R13	C RICHMOND	1
R13	H SANDUSKY	1
R13	G SUTHERLAND	3
R13	D TASKER	10
R13	W WILSON	1
R13	D WOODY	1
R13	C WONG	1
R13	F ZERILLI	1
R14		1
R14	R BARASH	1
R14	T FARLEY	1
R14	J GASPIN	1
R14	J KOENIG	1
R14	D LEHTO	1
R14	H MAIR	1
R14	P MONTANARO	1
R14	J POWELL	1
R14	M SWISDAK	1
R15		1
R16	B BAUDLER	1
R16	L HUDSON	1
R16	L MENSI	1
R16	L MONTESI	1
R16	T SPIVAK	1
R16	P WALTER	1
R31		1
R31	E BALIZER	1
R31	B HARTMANN	1
R31	W MADIGOSKY	1
R44		1
R44	W SZYMCZAK	1

REPORT DOCUMENTATION PAGE

Form Approved
OMB No. 0704-0188

1. AGENCY USE ONLY (Leave blank)	2. REPORT DATE	3. REPORT TYPE AND DATES COVERED
	16 February 1994	

4. TITLE AND SUBTITLE
PVDF Pressure Transducers for Shock Wave and Explosives Research

5. FUNDING NUMBERS

6. AUTHOR(S)
Paul Gustavson, Douglas Tasker, and Jerry Forbes

7. PERFORMING ORGANIZATION NAME(S) AND ADDRESS(ES)
Naval Surface Warfare Center (Code R13)
10901 New Hampshire Avenue
Silver Spring, MD 20903-5640

8. PERFORMING ORGANIZATION REPORT NUMBER
NAVSWC TR 91-506

9. SPONSORING/MONITORING AGENCY NAME(S) AND ADDRESS(ES)

10. SPONSORING/MONITORING AGENCY REPORT NUMBER

11. SUPPLEMENTARY NOTES

12a. DISTRIBUTION/AVAILABILITY STATEMENT
Approved for public release; distribution is unlimited.

12b. DISTRIBUTION CODE

13. ABSTRACT (Maximum 200 words)

A polyvinylidene fluoride (PVDF) piezoelectric pressure transducer is described in this report. Techniques for its use and experimental applications are described in detail.

14. SUBJECT TERMS
PVDF
Pressure Time Profiles
Charge Mode
Current Mode

15. NUMBER OF PAGES
60

16. PRICE CODE

17. SECURITY CLASSIFICATION OF REPORT	18. SECURITY CLASSIFICATION OF THIS PAGE	19. SECURITY CLASSIFICATION OF ABSTRACT	20. LIMITATION OF ABSTRACT
UNCLASSIFIED	UNCLASSIFIED	UNCLASSIFIED	SAR

GENERAL INSTRUCTIONS FOR COMPLETING SF 298

The Report Documentation Page (RDP) is used in announcing and cataloging reports. It is important that this information be consistent with the rest of the report, particularly the cover and its title page. Instructions for filling in each block of the form follow. It is important to ***stay within the lines*** to meet ***optical scanning requirements.***

Block 1. Agency Use Only *(Leave blank)*.

Block 2. Report Date. Full publication date including day, month, and year, if available (e.g. 1 Jan 88). Must cite at least the year.

Block 3. Type of Report and Dates Covered. State whether report is interim, final, etc. If applicable, enter inclusive report dates (e.g. 10 Jun 87 - 30 Jun 88).

Block 4. Title and Subtitle. A title is taken from the part of the report that provides the most meaningful and complete information. When a report is prepared in more than one volume, repeat the primary title, add volume number, and include subtitle for the specific volume. On classified documents enter the title classification in parentheses.

Block 5. Funding Numbers. To include contract and grant numbers; may include program element number(s), project number(s), task number(s), and work unit number(s). Use the following labels:

C	- Contract	PR	- Project
G	- Grant	TA	- Task
PE	- Program Element	WU	- Work Unit Accession No.

BLOCK 6. Author(s). Name(s) of person(s) responsible for writing the report, performing the research, or credited with the content of the report. If editor or compiler, this should follow the name(s).

Block 7. Performing Organization Name(s) and Address(es). Self-explanatory.

Block 8. Performing Organization Report Number. Enter the unique alphanumeric report number(s) assigned by the organization performing the report.

Block 9. Sponsoring/Monitoring Agency Name(s) and Address(es). Self-explanatory.

Block 10. Sponsoring/Monitoring Agency Report Number. *(If Known)*

Block 11. Supplementary Notes. Enter information not included elsewhere such as: Prepared in cooperation with...; Trans. of...; To be published in.... When a report is revised, include a statement whether the new report supersedes or supplements the older report.

Block 12a. Distribution/Availability Statement. Denotes public availability or limitations. Cite any availability to the public. Enter additional limitations or special markings in all capitals (e.g. NOFORN, REL, ITAR).

DOD	- See DoDD 5230.24, "Distribution Statements on Technical Documents."
DOE	- See authorities.
NASA	- See Handbook NHB 2200.2
NTIS	- Leave blank.

Block 12b. Distribution Code.

DOD	- Leave blank.
DOE	- Enter DOE distribution categories from the Standard Distribution for Unclassified Scientific and Technical Reports.
NASA	- Leave blank.
NTIS	- Leave blank.

Block 13. Abstract. Include a brief ***(Maximum 200 words)*** factual summary of the most significant information contained in the report.

Block 14. Subject Terms. Keywords or phrases identifying major subjects in the report.

Block 15. Number of Pages. Enter the total number of pages.

Block 16. Price Code. Enter appropriate price code ***(NTIS only)***

Blocks 17.-19. Security Classifications. Self-explanatory. Enter U.S. Security Classification in accordance with U.S. Security Regulations (i.e., UNCLASSIFIED). If form contains classified information, stamp classification on the top and bottom of the page.

Block 20. Limitation of Abstract. This block must be completed to assign a limitation to the abstract. Enter either UL (unlimited) or SAR (same as report). An entry in this block is necessary if the abstract is to be limited. If blank, the abstract is assumed to be unlimited.